

# Identification and Characterization of Keyhole Limpet Hemocyanin *N*-Glycans Mediating Cross-reactivity with *Schistosoma mansoni*<sup>\*§</sup>

Received for publication, June 1, 2005, and in revised form, August 15, 2005 Published, JBC Papers in Press, August 31, 2005, DOI 10.1074/jbc.M505985200

Hildegard Geyer<sup>‡</sup>, Manfred Wuhrer<sup>‡§</sup>, Anja Resemann<sup>¶</sup>, and Rudolf Geyer<sup>‡¶1</sup>

From the <sup>‡</sup>Institute of Biochemistry, Faculty of Medicine, University of Giessen, Friedrichstrasse 24, D-35392 Giessen, Germany, the

<sup>§</sup>Department of Parasitology, Center of Infectious Diseases, Leiden University Medical Center, P.O. Box 9600, NL-2300 RC Leiden, The Netherlands, and <sup>¶</sup>Bruker Daltonik GmbH, Fahrenheitstrasse 4, D-28359 Bremen, Germany

Keyhole limpet hemocyanin (KLH) of the mollusc *Megathura crenulata* is known to serologically cross-react with *Schistosoma mansoni* glycoconjugates in a carbohydrate-dependent manner. To elucidate the structural basis for this cross-reactivity, KLH glycans were released from tryptic glycopeptides and fluorescently labeled. Cross-reacting glycans were identified using a polyclonal antiserum reacting with soluble *S. mansoni* egg antigens, isolated by a three-dimensional fractionation scheme and analyzed by different mass spectrometric techniques as well as linkage analysis and exoglycosidase treatment. The results revealed that cross-reacting species comprise ~4.5% of released glycans. They all represent novel types of *N*-glycans with a Fuc( $\alpha$ 1–3)GalNAc( $\beta$ 1–4)[Fuc( $\alpha$ 1–3)]GlcNAc motif, which is known to occur also in schistosomal glycoconjugates. The tetrasaccharide unit is attached to the 3-linked antenna of a trimannosyl core, which can be further decorated by galactosyl residues, a xylose residue in 2-position of the central mannose and/or a fucose at the innermost *N*-acetylglucosamine. This study provides for the first time detailed structural data on the KLH carbohydrate entities responsible for cross-reactivity with glycoconjugates from *S. mansoni*.

Hemocyanins act as oxygen-transporting proteins in many arthropod and mollusc species (1). In addition to this biochemical function, the hemocyanin of the Californian giant keyhole limpet *Megathura crenulata*, a marine gastropod, is known to be a potent immunoactivator (for reviews, see Refs. 2 and 3). Due to these immunostimulatory properties, keyhole limpet hemocyanin (KLH)<sup>2</sup> is widely used in research and clinical studies. Present fields of application are, for example, immunotherapy of bladder cancer (4–7), based on the assumed expression of Gal( $\beta$ 1–3)GalNAc determinants as cross-reacting epitopes (8), and its use as a carrier of polysialic acid or low molecular weight haptens, such as synthetic oligosaccharides, gangliosides, or (glyco)peptides, designed

for potential application in anticancer therapy (9–14). Intriguingly, KLH has been further demonstrated to exhibit a carbohydrate-based cross-reactivity with glycoconjugates from *Schistosoma mansoni* (15) thus allowing the diagnosis of *S. mansoni* (6, 7, 16), *Schistosoma hematobium* (17), and *Schistosoma japonicum* (18) infections by enzyme-linked immunosorbent assay (ELISA). Hence, KLH has also been discussed as a potential candidate for vaccination against schistosomiasis (15). On the other hand, agarose beads coated with KLH or KLH-glycopeptides have been shown to mimic in a carbohydrate-dependent manner the hepatic granuloma formation mediated by *S. mansoni* eggs (19). Therefore, KLH may also be regarded as a model antigen to study the immunopathological mechanisms of schistosome infections.

Although it is generally accepted that the oligosaccharide constituents of KLH are of prime significance for its antigenicity and biomedical properties (2), knowledge on the carbohydrate structure of this glycoprotein is still incomplete. Structural studies performed so far revealed, however, that KLH is very heterogeneously glycosylated carrying preponderantly high mannose-type glycans with 5–7 mannosyl residues, hybrid-type species with five mannoses and one *N*-acetylglucosamine chain as well as truncated sugar chains derived thereof. As a unique feature, the latter glycans carry, in part, a Gal( $\beta$ 1–6)Man determinant, which has not been found in glycoprotein-*N*-glycans so far (20). Recent studies further demonstrated the presence of a novel type of *N*-glycans exhibiting Gal( $\beta$ 1–4)Fuc( $\alpha$ 1–6)- or Gal( $\beta$ 1–4)Gal( $\beta$ 1–4)Fuc( $\alpha$ 1–6)-core modifications (21).

Regarding KLH cross-reactivity with schistosomal glycoconjugates, a fucose-containing carbohydrate epitope could be identified in *S. mansoni* glycolipids (22), which comprises terminal Fuc( $\alpha$ 1–3)GalNAc units (23) and is obviously shared by keyhole limpet hemocyanin. Respective KLH glycans, however, have not been isolated and elucidated so far. To provide a rationale for the recognition of this glycoprotein by using *S. mansoni* infection sera as well as monoclonal or polyclonal antibodies reacting with schistosomal glycoconjugates, we have performed a detailed structural analysis focusing exclusively on the serologically cross-reacting carbohydrate moieties.

## EXPERIMENTAL PROCEDURES

**Materials**—KLH was either purchased from Sigma or kindly provided in purified form (Vacmune®, Biosyn Co., Fellbach, Germany) by J. Markl, Institute of Zoology, University of Mainz, Germany. Peptide *N*-glycosidase F (PNGase F) as well as  $\alpha$ -mannosidase from jack beans,  $\alpha$ -fucosidase from bovine kidney, and  $\beta$ -galactosidase from jack beans were obtained from Roche Diagnostics (Mannheim, Germany), Sigma, and Glyco (Upper Herford, UK), respectively. Agarose-*Aleuria aurantia* lectin (AAL) was purchased from Vector Laboratories (Burlingame, CA). Rabbit anti-soluble egg antigen (SEA) hyperimmune serum (24)

<sup>\*</sup> This work was supported by the Deutsche Forschungsgemeinschaft (Grants SFB535 and Ge386/3). The costs of publication of this article were defrayed in part by the payment of page charges. This article must therefore be hereby marked "advertisement" in accordance with 18 U.S.C. Section 1734 solely to indicate this fact.

<sup>§</sup> The on-line version of this article (available at <http://www.jbc.org>) contains supplemental Table S1 and Figs. S1 and S2.

<sup>1</sup> To whom correspondence should be addressed. Tel.: 49-641-99-47400; Fax: 49-641-99-47409; E-mail: Rudolf.Geyer@biochemie.med.uni-giessen.de.

<sup>2</sup> The abbreviations used are: KLH, keyhole limpet hemocyanin; CID, high energy collision-induced dissociation; dHex, deoxyhexose; ELISA, enzyme-linked immunosorbent assay; ESI, electrospray ionization; Hex, hexose; HexNAc, *N*-acetylhexosamine; IT, ion trap; LC, liquid chromatography; LID, laser-induced dissociation; MALDI-TOF, matrix-assisted laser desorption/ionization time-of-flight; MS, mass spectrometry; MS/MS, tandem mass spectrometry; PA, pyridylamine (2-aminopyridine); PBS, phosphate-buffered saline; Pent, pentose; PNGase F, peptide *N*-glycosidase F; TBS, Tris-buffered saline; SEA, soluble egg antigen; HPLC, high performance liquid chromatography; AAL, *A. aurantia* lectin.

## KLH Cross-reacting Carbohydrate Epitopes

was a generous gift of M. J. Doenhoff, School of Biological Sciences, University of Wales, Bangor, UK. Anti-SEA antibodies, coupled to NHS-activated Sepharose, were provided by T. Lehr, Institute of Biochemistry, University of Giessen. The monoclonal antibody M2D3H was produced and kindly provided by Q. Bickle, London School of Hygiene and Tropical Medicine, London University, UK (25).

**Enzyme-linked Immunosorbent Assay**—KLH tryptic (glyco-)peptides were assayed by ELISA with/without defucosylation by hydrogen fluoride (HF) treatment (see below). The (glyco-)peptides were adsorbed (200 ng per well in 100  $\mu$ l of 0.1 M Na<sub>2</sub>CO<sub>3</sub>, pH 9.6, 2 h at 37 °C) to microtiter plates (Maxisorb, Nunc, Wiesbaden, Germany). Plates were washed twice with Tris-buffered saline (TBS, 25 mM Tris-HCl, pH 7.5, 100 mM sodium chloride). Plates were blocked for 1 h with 0.5% bovine serum albumin in TBS. Incubation with 100  $\mu$ l per well of the primary antibody in TTBS-10 (TBS 1:10 diluted, 0.05% Tween 20) containing 0.25% bovine serum albumin was performed for 1 h at 37 °C. Primary antibodies used were: monoclonal antibody M2D3H (ascites fluid, dilution 1:100,000 (25)), murine *S. mansoni* infection serum (dilution 1:2,000), an anti-KLH rabbit hyperimmune serum ( $\alpha$ KLH, dilution 1:100,000 (22)), and an anti-soluble egg antigen rabbit hyperimmune serum ( $\alpha$ SEA, dilution 1:100,000 (24)). After multiple washes with TTBS-10, alkaline phosphatase-conjugated goat anti-mouse Ig (Dako Diagnostics, Hamburg, Germany, diluted 1:1,000) or goat anti-rabbit Ig (Sigma, diluted 1:1,000) in TTBS-10 containing 0.25% bovine serum albumin were applied. Plates were washed with TTBS-10 and incubated with 0.1% *p*-nitrophenyl phosphate (Biomol, Hamburg, Germany) in 100 mM glycine buffer, pH 10.4, containing 1 mM ZnCl<sub>2</sub>, and 1 mM MgCl<sub>2</sub> at 37 °C. After 30 min, absorption at 405 nm was determined.

**Isolation of Oligosaccharides**—Tryptic glycopeptides were subjected to hydrazinolysis (26, 27) or treated with PNGase F as described previously (21). The resulting mixture of products was applied to a reverse-phase cartridge (C18ec, Macherey und Nagel, Düren, Germany). Released oligosaccharides were recovered in the flow-through and were collected. For desalting, glycans were applied to a porous graphitic-carbon cartridge (Supelclean ENVI-Carb, Supelco, Bellefonte, PA). The cartridges were washed with water, and oligosaccharides were eluted with 25% (v/v) aqueous acetonitrile.

**Separation of Pyridylaminated Oligosaccharides**—Released oligosaccharides were labeled with 2-aminopyridine according to Kuraya *et al.* (27). PA-oligosaccharides were preparatively fractionated on an amino-phase HPLC column (4.6  $\times$  250 mm, Nucleosil-Carbohydrate, Macherey und Nagel) at a flow rate of 1 ml/min at room temperature and detected by fluorescence (310/380 nm) (28). The column was equilibrated with 200 mM aqueous triethylamine/acetic acid, pH 7.3:acetonitrile (25:75, v/v). A gradient of 25% to 60% 200 mM aqueous triethylamine/acetic acid buffer in acetonitrile was applied within a 60-min period. Elution was continued under isocratic conditions for a further 10 min. Peak fractions were collected and lyophilized.

Obtained oligosaccharide fractions were applied to a column filled with 10 ml of *A. aurantia* lectin (AAL)-agarose, which had been equilibrated with phosphate-buffered saline (PBS, 6.5 mM KH<sub>2</sub>PO<sub>4</sub>, 0.15 M NaCl, pH 7.4). The column was eluted with 50 ml of PBS, 30 ml of PBS containing 1 mM fucose, and 30 ml of PBS containing 50 mM fucose. Fractions of 10 ml were collected and lyophilized.

For further preparative separation, oligosaccharides were, in part, subfractionated onto an ODS-Hypersil C<sub>18</sub> column (3  $\mu$ m, 0.46  $\times$  15 cm, Shandon, UK) at 40 °C at a flow rate of 1 ml/min. The column was equilibrated with 50 mM triethylamine/acetic acid, pH 5.0. A gradient from 0% to 50% 50 mM triethylamine/acetic acid, pH 5.0/0.5% 1-butanol was applied over 50 min. PA-oligosaccharides were detected by fluores-

cence using an excitation wavelength of 320 nm and an emission wavelength of 400 nm (28).

**Immunoaffinity Chromatography**—Anti-SEA-Sepharose (1 ml) was packed into a column of 8-mm diameter and washed with TBS (25 mM Tris/HCl, pH 7.5, 100 mM NaCl). PA-oligosaccharides were applied to the column in 150  $\mu$ l of TBS, followed by 1-h incubation at room temperature. After washing the column with 10 ml of TBS, bound PA-oligosaccharides were eluted with 2 ml of 100 mM triethylamine, pH 11.5, 150 mM NaCl. Both flow-through and eluate were applied separately to a 25-mg porous graphitic-carbon cartridge (Thermoquest, Kleinstheim, Germany) for desalting. The cartridge was washed with 10 ml of water, and PA-oligosaccharides were eluted with 5 ml of 25% (v/v) aqueous acetonitrile. Samples were dried in a Speed-Vac concentrator.

**Matrix-assisted Laser-desorption Ionization Time-of-flight Mass Spectrometry**—MALDI-MS was performed either on a Vision 2000 instrument (ThermoFinnigan, Eggenstein, Germany) equipped with a UV nitrogen laser (337 nm) or on an Ultraflex TOF/TOF mass spectrometer (Bruker Daltonik GmbH, Bremen, Germany) equipped with a LIFT-MS/MS facility. The instruments were operated in the positive-ion reflectron mode using 6-aza-2-thiothymine (Sigma) as matrix (20, 21). Measurements with the Vision 2000 instrument allowed the determination of average masses only, whereas isotopic resolution was achieved with the Ultraflex mass spectrometer. Fragment ion analysis by tandem mass spectrometry (MS/MS) after laser-induced dissociation (LID) was performed as detailed earlier (21).

For high energy collision-induced dissociation (CID) experiments, a 5 mg/ml solution of 2,5-dihydroxybenzoic acid (Sigma) in 30% acetonitrile in 0.1% trifluoroacetic acid was prepared. About 1–2  $\mu$ l of glycan sample and 0.5  $\mu$ l of matrix solution were applied to an 800- $\mu$ m hydrophilic anchor of an AnchorChip<sup>TM</sup> MALDI sample plate (Bruker) and dried by a cold air stream resulting in a typical preparation with large heterogeneous crystals at the rim and a more homogeneous thin crystal layer in the center of the spot. From this central region, exclusively sodiated glycan ions were obtained and selected for further MS/MS experiments. The CID spectra were obtained by using an Ultraflex TOF/TOF II instrument (Bruker) using the LIFT device for selection and fragmentation of the sodiated glycan ions as described before (29, 30). Acceleration voltage in the ion source was 8 kV, the Timed Ion Selector was set to 0.4% (relative to parent mass), and argon was used as collision gas ( $\sim 4\text{--}6 \times 10^{-6}$  mbar). Resulting fragments were further accelerated in a second source by 19 kV and analyzed by a two-stage gridless reflectron. In addition, a new all solid state laser system called SmartBeam<sup>TM</sup> was used allowing a 200-Hz acquisition of high quality spectra from all matrix and preparation types comparable to the quality obtainable with N<sub>2</sub> lasers. Typically, 200 shots were accumulated for the parent ion signal and 1000–2000 shots for the fragments. Compass 1.1 consisting of FlexControl 2.4, and FlexAnalysis 2.4 was used as instrument control and processing software.

**Nano-LC-Electrospray Ionization-Ion Trap-Mass Spectrometry**—N-Glycans were separated on a nanoscale Amide-80 column (5  $\mu$ m, 80  $\times$  75  $\mu$ m  $\times$  100 mm, Tosoh, Montgomeryville, PA) as outlined previously for native oligosaccharides (31). The system was directly coupled with an Esquire HCT ESI-IT-MS (Bruker) equipped with an online nanospray source operating in the positive-ion mode. For electrospray (900–1200 V), capillaries (360  $\mu$ m out diameter, 20  $\mu$ m inner diameter with 10- $\mu$ m opening) from New Objective (Cambridge, MA) were used. The solvent was evaporated at 120 °C with a nitrogen stream of 6 liters/min. Ions from *m/z* 50 to *m/z* 2500 were registered.

**Enzymatic and Chemical Degradation**—PA-oligosaccharides were treated with  $\alpha$ -fucosidase from bovine kidney (4 milliunits/ $\mu$ l, Roche

Diagnostics) directly on the MALDI-MS target (32). The enzyme was dialyzed for 2 h against 25 mM ammonium acetate, pH 5. After measurement of the educts by MALDI-MS, the dialyzed enzyme (1  $\mu$ l) was added to samples on the target, and spots were analyzed again by MALDI-MS after overnight incubation at 37 °C. Digestions with  $\beta$ -galactosidase,  $\alpha$ -mannosidase, or  $\beta$ -N-acetylhexosaminidase from jack beans as well as  $\alpha$ -galactosidase from green coffee beans were performed with 1  $\mu$ l of the respective dialyzed enzymes in the same manner. For chemical defucosylation, dried samples were treated with 48% HF at 4 °C overnight (modified from Ref. 33). HF was removed by a stream of nitrogen. The anomeric configuration of fucosyl and galactosyl residues was determined by chromium trioxide oxidation (34).

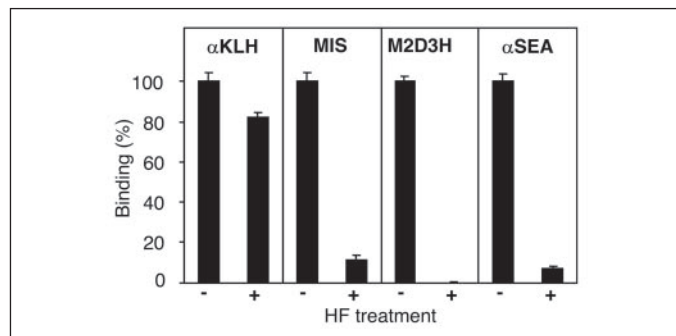


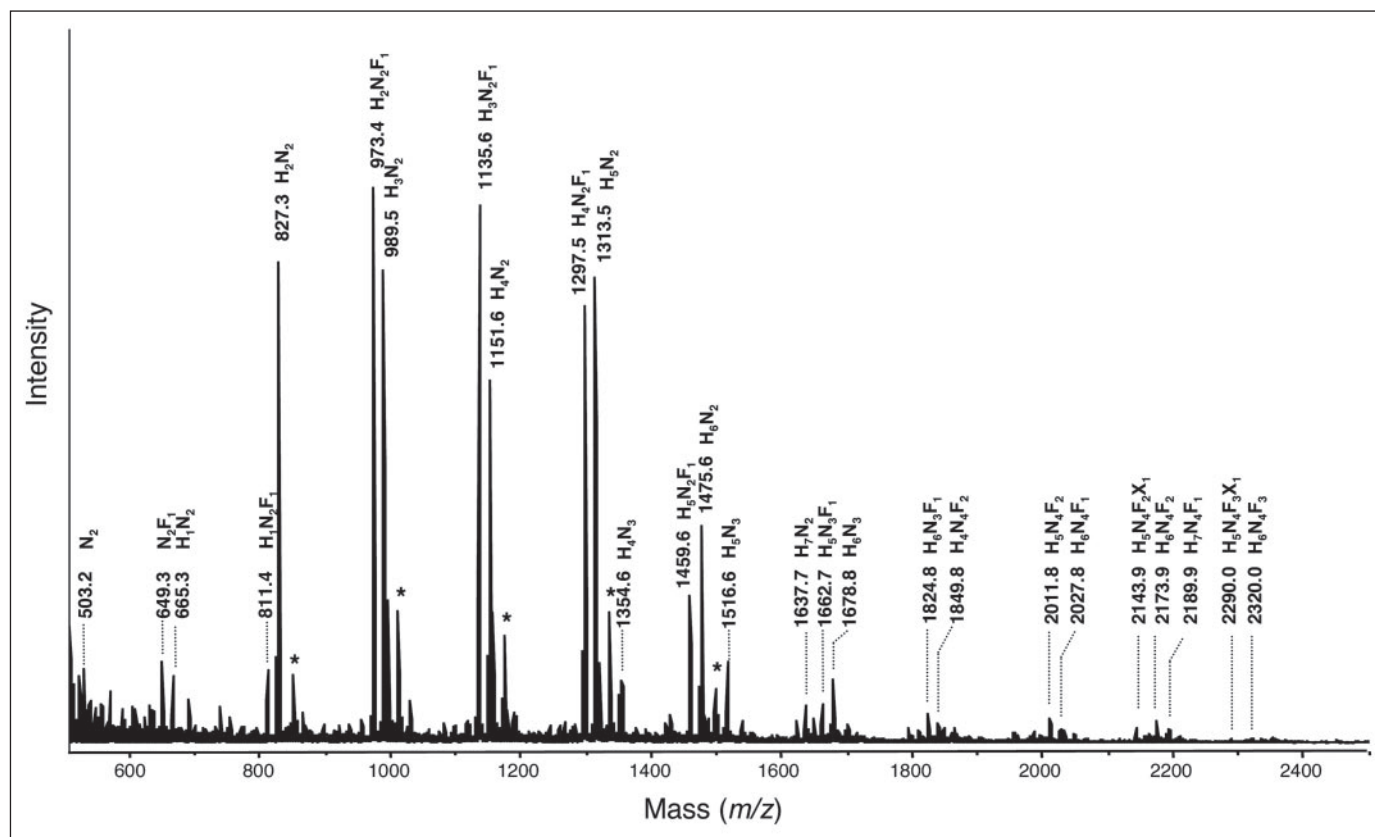
**FIGURE 1. Antibody recognition of fucosylated antigens on KLH by *S. mansoni*-reactive antibodies.** KLH tryptic peptides before (–) and after (+) HF treatment were assayed by ELISA for their recognition by various antibodies, including a rabbit hyperimmune serum raised against KLH ( $\alpha$ KLH), pooled murine *S. mansoni* infection sera (MIS), the monoclonal antibody M2D3H, and a rabbit hyperimmune serum raised against schistosomal soluble egg antigens ( $\alpha$ SEA). Mean values of six measurements are given with bars indicating standard deviations. Results for glycopeptides before HF treatment were defined as 100%.

**Monosaccharide Composition and Linkage Analysis**—After hydrolysis in 4 N aqueous trifluoroacetic acid at 100 °C for 4 h and labeling with anthranilic acid, monosaccharides were determined by HPLC, and fluorescence detection (34, 35). For linkage analysis, PA-oligosaccharides were permethylated and hydrolyzed. Partially methylated alditol acetates obtained after sodium borohydride reduction and peracetylation were analyzed by capillary GLC/MS in the chemical ionization as well as electron impact ionization mode using the instrumentation and micro-techniques described elsewhere (36, 37).

## RESULTS

**Isolation of KLH Oligosaccharides Sharing Carbohydrate Epitopes with *S. mansoni* Glycoconjugates**—KLH exhibits, in part, oligosaccharide moieties, which are serologically cross-reacting with *S. mansoni* carbohydrate antigens. Using ELISA as assay system, KLH glycopeptides were recognized by murine *S. mansoni* infection sera, the monoclonal antibody M2D3H reacting with the Fuc( $\alpha$ 1–3)GalNAc-epitope (23) and polyclonal antibodies raised against SEA of *S. mansoni* (Fig. 1). In contrast to rabbit hyperimmune serum raised against KLH, antibody binding was mostly eliminated by mild HF treatment, which results in a release of fucose residues leaving the remaining carbohydrate chains largely intact (23). In agreement with previous data (22) it may be, therefore, concluded that cross-reacting oligosaccharides comprise a fucosylated carbohydrate epitope. Furthermore, this experiment established rabbit polyclonal anti-SEA serum as a suitable tool for the identification of cross-reactive KLH glycan species.

To isolate these carbohydrates in a preparative scale for structural studies, KLH glycopeptides were subjected to hydrazinolysis or treatment with PNGase F. Released oligosaccharides were fluorescently labeled by reductive amination with 2-aminopyridine and analyzed by MALDI-MS (Fig. 2).



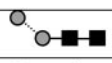
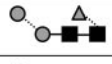
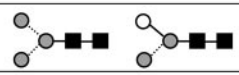
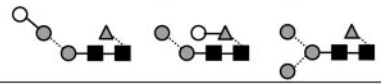
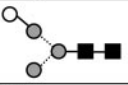
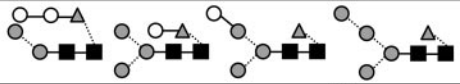
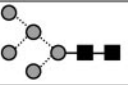
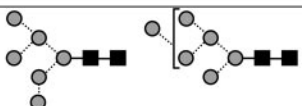
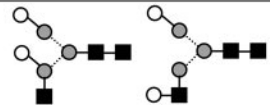
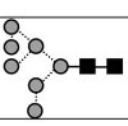
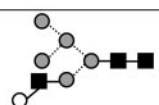
**FIGURE 2. MALDI-MS analysis of total KLH-derived PA-oligosaccharides.** Deduced monosaccharide compositions are assigned to the pseudomolecular ions  $[M+H]^+$  recorded with isotopic resolution. Corresponding sodium adducts are marked by asterisks. H, hexose; N, N-acetylhexosamine; F, deoxyhexose (fucose); X, pentose (xylose).



TABLE ONE

**Compilation of total KLH-derived PA-glycans registered by MALDI-MS**

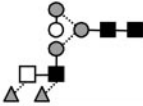
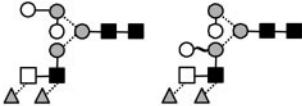
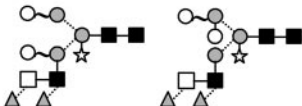
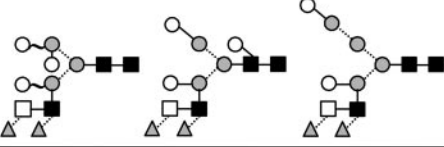
Compositions are assigned in terms of hexose (H), *N*-acetylhexosamine (N), deoxyhexose (fucose; F) and pentose (xylose; X). Relative occurrence of individual compositional species is roughly estimated from the respective signal intensities. Published KLH glycan structures and corresponding references are included. Compositional species serological cross-reacting with *S. mansoni* glycoconjugates are given in bold and italics.

Measured mass <sup>a</sup> [M+H] <sup>+</sup> ([M+Na] <sup>+</sup> )	Composition				Oligosaccharide structure <sup>b</sup>	Occurrence <sup>c</sup>	Reference
	H	N	F	X			
503.2		2				+	
649.3		2	1			+	
665.3	1	2				+	
811.4	1	2	1			+	
827.3	2	2				+++	(20,21)
973.4	2	2	1			+++++	(20,21)
989.5	3	2				++++	(20)
1135.6	3	2	1			+++++	(20,21)
1151.6	4	2				+++	(20)
1297.5	4	2	1			++++	(20,21)
1313.5	5	2				+++++	(20)
1429.5	4	2	1	1		(+)	
1459.6	5	2	1			++	
1475.6	6	2				+++	(20)
1500.6	4	3	1			(+)	
1516.6	5	3				+	(20)
1621.6	6	2	1			(+)	
1637.7 (1660.5)	7	2				(+)	(20)
1648.6	5	3		1		(+)	
1662.7 (1685.6)	5	3	1			(+)	
<b>1671.9</b>	<b>2</b>	<b>4</b>	<b>3</b>			- <sup>d</sup>	
1678.8 (1701.5)	6	3				+	(20)
<b>1687.9 (1710.7)</b>	<b>3</b>	<b>4</b>	<b>2</b>			- <sup>d</sup>	

In agreement with previous studies, mass spectrometry revealed a highly heterogeneous mixture of different glycans comprising at least 50 different compositional species with monosaccharide compositions of Hex<sub>0-9</sub>HexNAc<sub>2-4</sub>dHex<sub>0-3</sub>Pent<sub>0-1</sub>, the deoxyhexose and pentose residues of which represented exclusively fucose (20) and xylose (see below), respectively (TABLE ONE). Previous studies (20, 21) focusing mainly on the major, non-cross-reactive sugar chains of KLH have already dem-

onstrated that individual compositional species are frequently representing different isomeric and/or isobaric structures (see, for example, structures of Hex<sub>3</sub>HexNAc<sub>2</sub>, Hex<sub>3</sub>HexNAc<sub>2</sub>Fuc<sub>1</sub>, Hex<sub>4</sub>HexNAc<sub>2</sub>Fuc<sub>1</sub>, and Hex<sub>5</sub>HexNAc<sub>3</sub> compounds in TABLE ONE), demonstrating again the vast heterogeneity of KLH glycosylation. Intriguingly, minor species, comprising <5% of the total glycans, could be additionally registered in the higher mass range (see Fig. 2), which contained more than one fucose and thus

TABLE ONE—CONTINUED

Measured mass <sup>a</sup> [M+H] <sup>+</sup> ([M+Na] <sup>+</sup> )	Composition				Oligosaccharide structure <sup>b</sup>	Occurrence <sup>c</sup>	Reference
	H	N	F	X			
1794.7 (1817.7)	5	3	1	1		(+)	
1799.7	8	2				(+)	
1808.7 (1831.7)	5	3	2			- <sup>d</sup>	
1824.8 (1847.7)	6	3	1			(+)	
<b>1833.9 (1856.7)</b>	<b>3</b>	<b>4</b>	<b>3</b>			(+)	
1840.7 (1863.8)	7	3				(+)	
<b>1849.8 (1872.9)</b>	<b>4</b>	<b>4</b>	<b>2</b>			(+)	this paper
1865.7 (1888.6)	5	4	1			(+)	
1956.7 (1980.0)	6	3	1	1		(+)	
1961.7 (1985.0)	9	2				(+)	
<b>1981.9</b>	<b>4</b>	<b>4</b>	<b>2</b>	<b>1</b>		- <sup>d</sup>	
1986.7 (2009.9)	7	3	1			(+)	
<b>1995.9 (2019.9)</b>	<b>4</b>	<b>4</b>	<b>3</b>			(+)	
<b>2011.8 (2034.9)</b>	<b>5</b>	<b>4</b>	<b>2</b>			(+)	this paper
2027.8 (2050.9)	6	4	1			(+)	
<b>2127.8 (2151.2)</b>	<b>4</b>	<b>4</b>	<b>3</b>	<b>1</b>		- <sup>d</sup>	
<b>2143.9 (2167.2)</b>	<b>5</b>	<b>4</b>	<b>2</b>	<b>1</b>		(+)	this paper
<b>2157.8 (2181.3)</b>	<b>5</b>	<b>4</b>	<b>3</b>			(+)	
<b>2173.9 (2197.2)</b>	<b>6</b>	<b>4</b>	<b>2</b>			+	this paper
2189.9 (2213.0)	7	4	1			(+)	
<b>2290.0 (2313.2)</b>	<b>5</b>	<b>4</b>	<b>3</b>	<b>1</b>		(+)	
2305.9 (2329.2)	6	4	2	1		- <sup>d</sup>	
<b>2320.0 (2343.2)</b>	<b>6</b>	<b>4</b>	<b>3</b>			(+)	
2335.9 (2359.2)	7	4	2			(+)	
2351.9	8	4	1			(+)	
<b>2451.9</b>	<b>6</b>	<b>4</b>	<b>3</b>	<b>1</b>		(+)	
<b>2482.0</b>	<b>7</b>	<b>4</b>	<b>3</b>			(+)	

<sup>a</sup> Proton adducts are given as monoisotopic; sodium adducts as average masses.

<sup>b</sup> Key symbols used for constituent monosaccharides: ○ = Man, ○ = Gal, □ = GalNAc, ■ = GlcNAc, ▲ = Fuc, ☆ = Xyl. Solid lines represent β-linkages, dashed lines are α-linkages, and wavy lines (—) are unassigned linkages. The bond angles indicate the linkage positions (40,62).

<sup>c</sup> (+) to +++++; 0–1,600, 1,601–4,000, 4,001–8,000, 8,001–12,000, 12,001–16,000, and 16,001–20,000 area counts, respectively.

<sup>d</sup> Only detectable after HPLC subfractionation, immunoaffinity chromatography, and/or lectin (AAL) affinity enrichment.

represented potential candidates for serological cross-reactivity with schistosomal glycans. To identify and verify such cross-reacting oligosaccharides, an aliquot of the total KLH-derived PA-glycans was subjected in analytical scale to immunoaffinity chromatography employing immobilized polyclonal anti-SEA antibodies. Subsequent analyses by MALDI-MS revealed the presence of 15 cross-reacting species with monosaccharide compositions of Hex<sub>2–7</sub>HexNAc<sub>4</sub>Fuc<sub>2–3</sub>Xyl<sub>0–1</sub> (Fig. 3) among which

Hex<sub>4</sub>HexNAc<sub>4</sub>Fuc<sub>2</sub>, Hex<sub>5</sub>HexNAc<sub>4</sub>Fuc<sub>2</sub>, Hex<sub>5</sub>HexNAc<sub>4</sub>Fuc<sub>2</sub>Xyl<sub>1</sub>, and Hex<sub>6</sub>HexNAc<sub>4</sub>Fuc<sub>2</sub> represented major species. Monofucosylated glycans did not bind to the immunoaffinity matrix.

For isolation and fractionation of the cross-reacting carbohydrate species PA-glycans were separated by HPLC on an aminophase column (Fig. 4A). Resulting oligosaccharide fractions were analyzed by MALDI-MS, which demonstrated that all of them still comprised heterogeneous

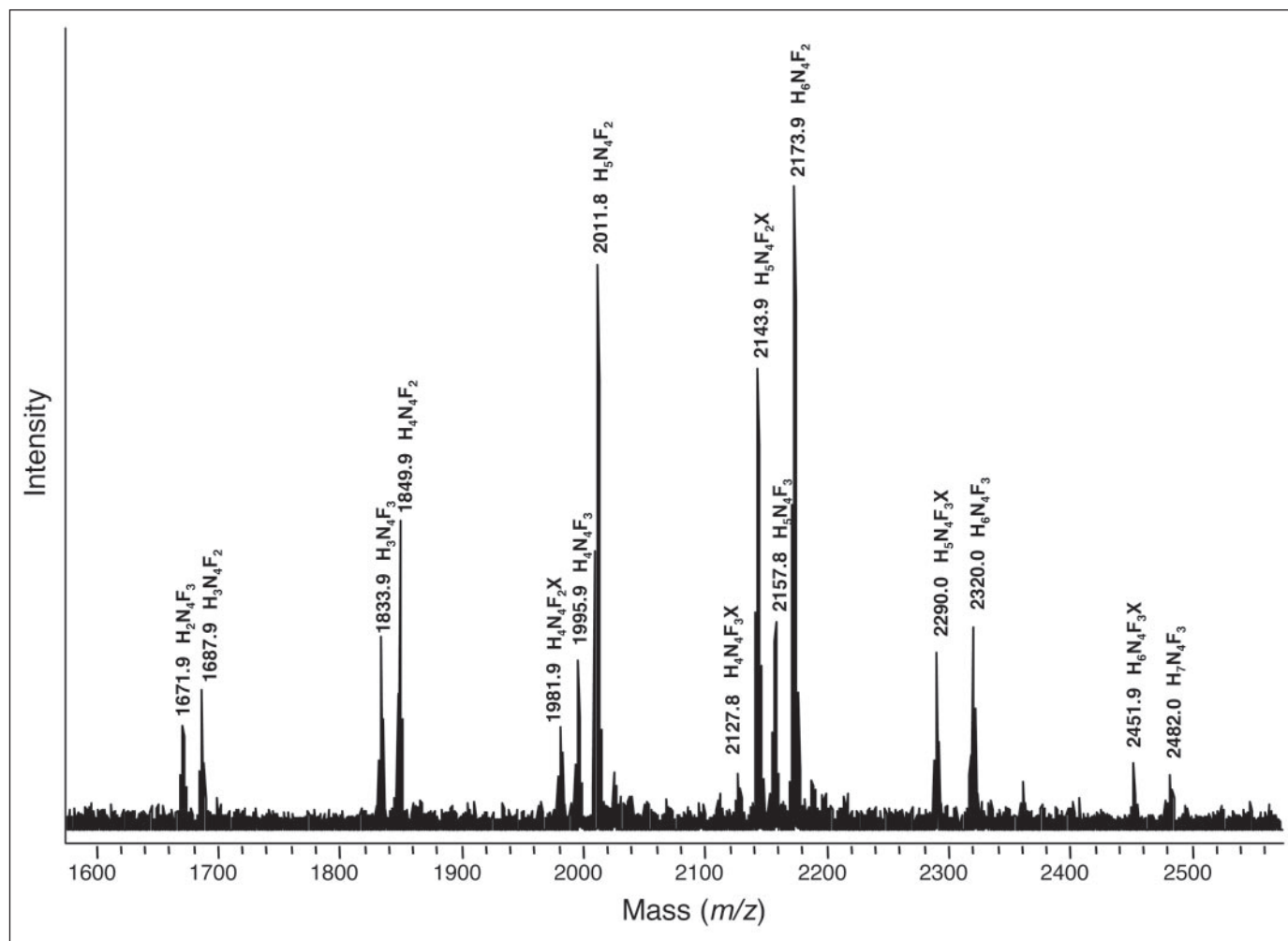


FIGURE 3. **Immunoaffinity chromatography of PA-oligosaccharides derived from KLH.** An aliquot of total PA-glycans was applied to an anti-soluble egg antigens ( $\alpha$ SEA) immunoaffinity column. Bound glycans were eluted as described under "Experimental Procedures" and analyzed by MALDI-MS. Protonated pseudomolecular ions  $[M+H]^+$  were registered with isotopic resolution. H, hexose; N, N-acetylhexosamine; F, fucose; X, xylose.

glycan mixtures (see, for example, Fig. 4, B–E). Obviously, efficient size fractionation of these oligosaccharides by aminophase HPLC could not be achieved possibly due to the great structural variability within one type of compositional species. Serologically cross-reacting oligosaccharides with more than one fucose constituent (Fig. 3) occurred preponderantly in fractions 12–15 (Fig. 4, B–E). Careful inspection of the highly complex MALDI-MS spectrum of fraction 11 glycans revealed no evidence for the presence of difucosylated oligosaccharides species, whereas the eluate recovered after fraction 15 was found to contain trace amounts of trifucosylated glycans with six to seven hexoses and, in part, one xylose residue that were not further analyzed. The obtained MALDI-MS spectra further demonstrated that the respective oligosaccharides represented often only minor constituents of these fractions.

To enrich these fucosylated oligosaccharides, relevant HPLC fractions 12–15 (Fig. 4A) were subjected in preparative scale to lectin affinity chromatography using immobilized *A. aurantia* lectin (AAL). Unbound glycans appearing in the flow-through as well as weakly and tightly bound oligosaccharide species, sequentially eluted with 1 mM and 50 mM fucose in PBS, were separately collected and analyzed by MALDI-MS. As shown in Fig. 5, oligosaccharides with two fucosyl residues and compositions of Hex<sub>3</sub>HexNAc<sub>4</sub>Fuc<sub>2</sub> ( $m/z$  1710.7), Hex<sub>4</sub>HexNAc<sub>4</sub>Fuc<sub>2</sub> ( $m/z$  1872.9), Hex<sub>5</sub>HexNAc<sub>4</sub>Fuc<sub>2</sub> ( $m/z$  2035.1), Hex<sub>5</sub>HexNAc<sub>4</sub>Fuc<sub>2</sub>Xyl<sub>1</sub> ( $m/z$  2167.1), and Hex<sub>6</sub>HexNAc<sub>4</sub>Fuc<sub>2</sub> ( $m/z$

2197.1) were primarily recovered in the weakly bound glycan fraction eluted with 1 mM Fuc (Fig. 5, A–D). Trifucosylated oligosaccharide species with compositions of Hex<sub>3</sub>HexNAc<sub>4</sub>Fuc<sub>3</sub> ( $m/z$  1856.7), Hex<sub>4</sub>HexNAc<sub>4</sub>Fuc<sub>3</sub> ( $m/z$  2019.0), Hex<sub>4</sub>HexNAc<sub>4</sub>Fuc<sub>3</sub>Xyl<sub>1</sub> ( $m/z$  2151.2), Hex<sub>5</sub>HexNAc<sub>4</sub>Fuc<sub>3</sub> ( $m/z$  2181.1), Hex<sub>5</sub>HexNAc<sub>4</sub>Fuc<sub>3</sub>Xyl<sub>1</sub> ( $m/z$  2313.2), and Hex<sub>6</sub>HexNAc<sub>4</sub>Fuc<sub>3</sub> ( $m/z$  2343.2) occurred preponderantly in the 50 mM fucose eluate (Fig. 5, E–H). The latter oligosaccharides, however, represented minor compounds as may be judged from the differences in signal intensities in the mass spectra shown in Fig. 5, although similar aliquots of the glycan fractions have been applied in both cases. Cross-reacting compositional species occurring only in trace amounts in the immunoaffinity eluate (see, for example, Hex<sub>2</sub>HexNAc<sub>4</sub>Fuc<sub>3</sub>, Hex<sub>4</sub>HexNAc<sub>4</sub>Fuc<sub>2</sub>Xyl<sub>1</sub>, Hex<sub>7</sub>HexNAc<sub>4</sub>Fuc<sub>3</sub>, or Hex<sub>6</sub>HexNAc<sub>4</sub>Fuc<sub>3</sub>Xyl<sub>1</sub> in Fig. 3) were not recovered probably due to small amounts as well as the fact that fraction 11 glycans and larger species being eluted after fraction 15 from the aminophase column have not been included.

Glycans obtained from aminophase HPLC fractions 12–15 (Fig. 4A) in the 1 mM Fuc eluate after lectin affinity chromatography (Fig. 5, A–D) were separately subjected to preparative reverse-phase HPLC for further fractionation (Fig. 6). Resulting subfractions were again analyzed by MALDI-MS. The results revealed that some of them still represented mixtures of oligosaccharides. In part, species with identical molecular

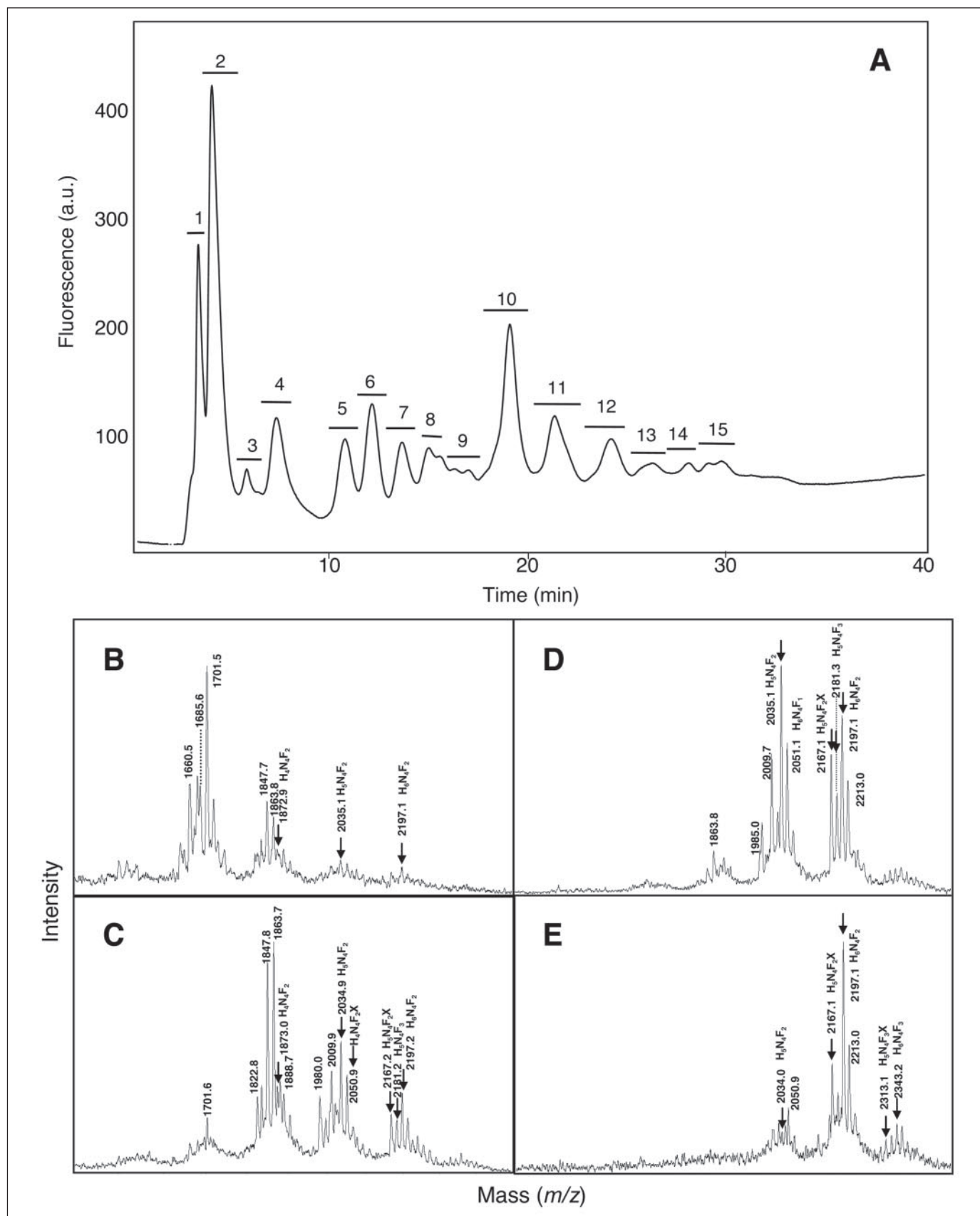


FIGURE 4. **Fractionation of PA-oligosaccharides.** A, PA-glycans were separated by HPLC using an aminophase column. Glycan fractions were numbered and separately pooled as indicated by horizontal bars. B–E, MALDI-MS spectra of oligosaccharides recovered in HPLC fractions 12–15, respectively. Average masses of sodiated pseudomolecular ions  $[M+Na]^+$  were registered. Cross-reacting species are marked by arrows, and respective monosaccharide compositions are given. For assignment of non-cross-reacting compounds see TABLE ONE. H, hexose; N, N-acetylhexosamine; F, fucose; X, xylose.

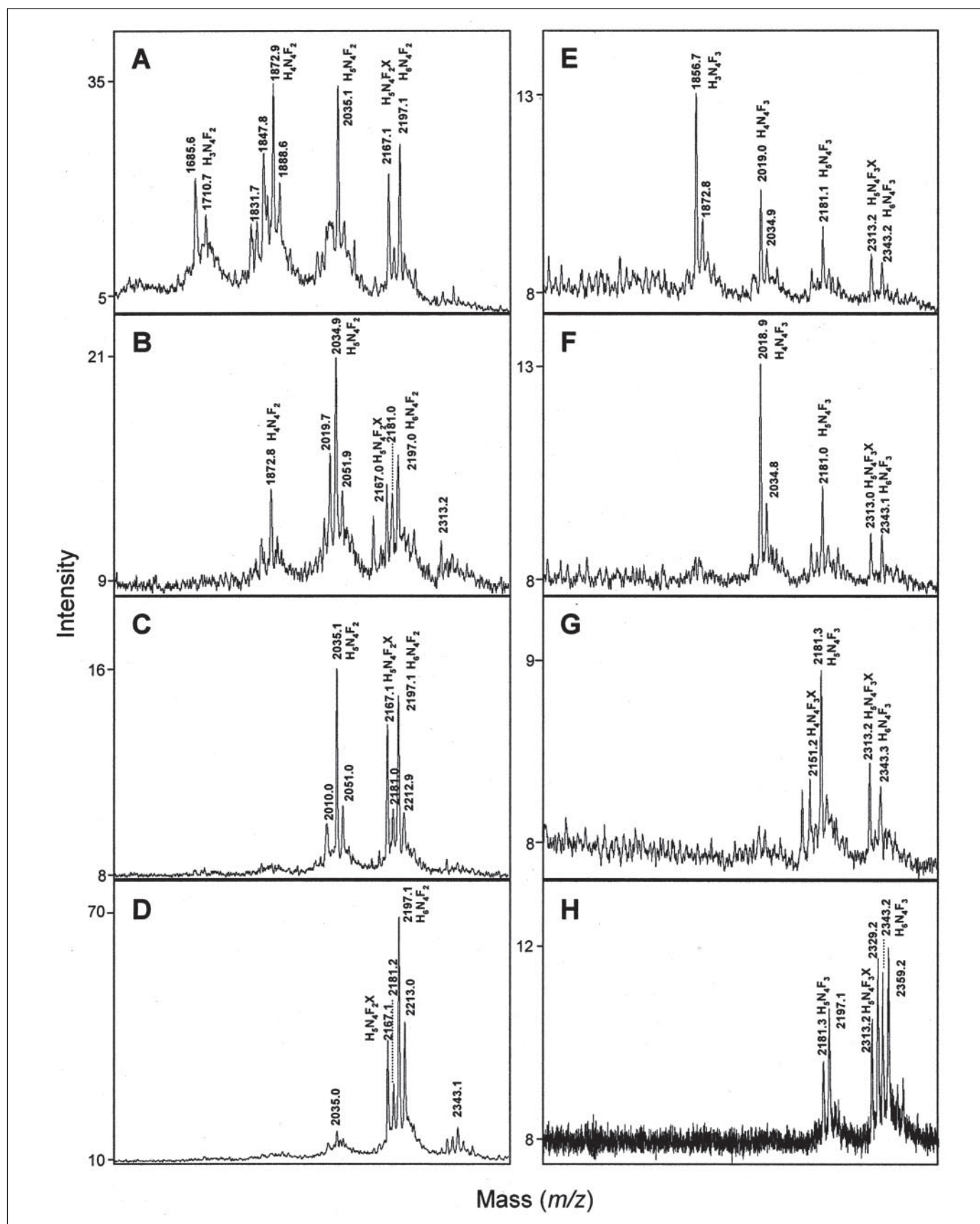


FIGURE 5. **Fractionation of KLH-derived PA-oligosaccharides by lectin affinity chromatography.** PA-glycans obtained in aminophase HPLC fractions 12–15 (cf. Fig. 4A) were individually loaded onto a column of immobilized *A. aurantia* lectin (AAL). A–D, weakly bound glycans of fractions 12–15 eluted with 1 mM Fuc, and E–H, tightly bound species of fractions 12–15 recovered with 50 mM Fuc, respectively. Obtained oligosaccharides were analyzed by MALDI-MS. Average masses of sodiated pseudomolecular ions  $[M+Na]^+$  are assigned together with monosaccharide compositions of cross-reacting species. H, hexose; N, N-acetylhexosamine; F, fucose; X, xylose.



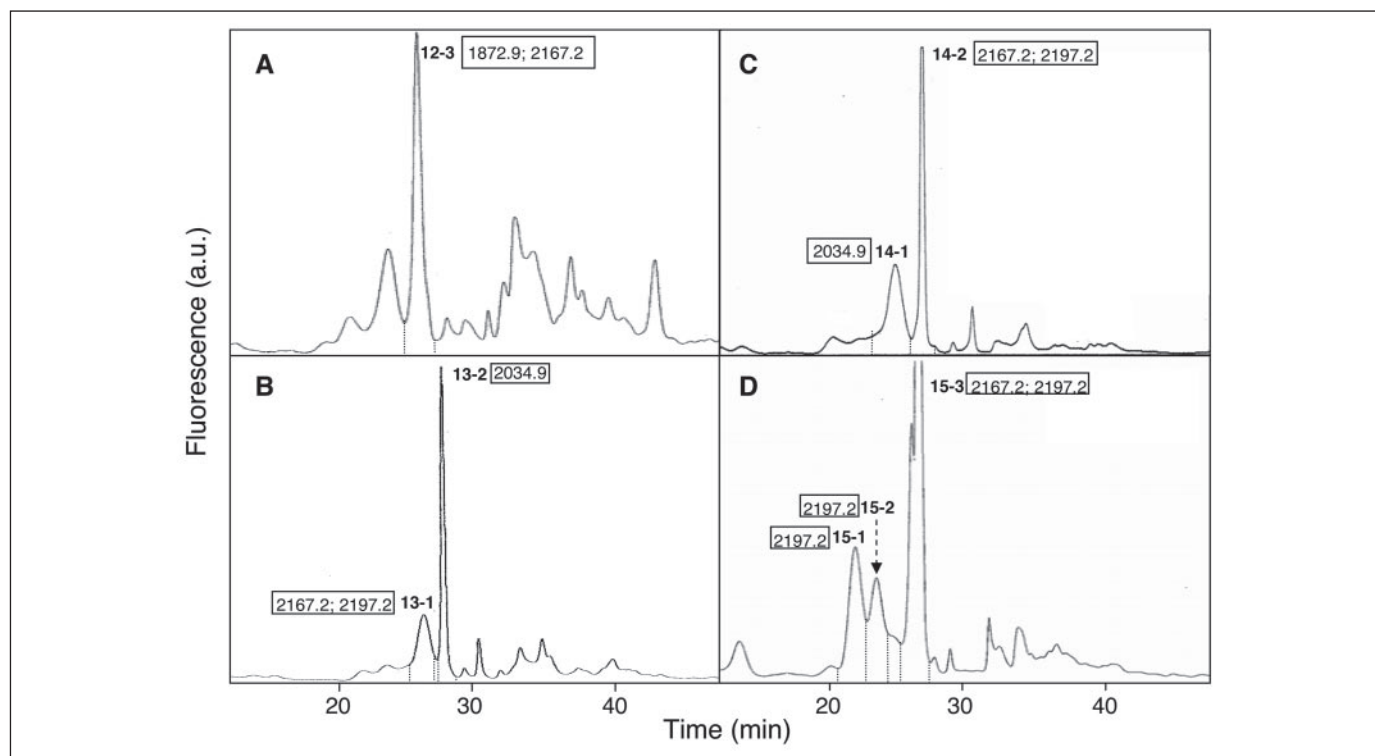


FIGURE 6. **Subfractionation of KLH-derived PA-oligosaccharides by reverse-phase HPLC.** Glycans obtained by aminophase HPLC (fractions 12–15) and subsequent lectin affinity chromatography (1 mM Fuc eluate) were individually subfractionated by reverse-phase HPLC. A–D, chromatographic profiles obtained for fractions 12–15, respectively. Resulting oligosaccharide subfractions were numbered and pooled as indicated. Average masses of major sodiated pseudomolecular ions  $[M+Na]^+$  registered by MALDI-MS analysis of individual subfractions are assigned.

masses also occurred in different fractions (Fig. 6, A–D). Hence, it has to be concluded that these glycans represent isomeric or isobaric variants.

To verify that the isolated glycan fractions comprised serologically cross-reacting oligosaccharide species, aliquots of fractions 12-3, 13-1, 13-2, 14-1, 14-2, 15-1, 15-2, and 15-3 were combined and subjected to immunoaffinity chromatography using immobilized polyclonal anti-SEA antibodies. Starting glycans, unbound material obtained in the flow-through, and oligosaccharides recovered in the immunoaffinity eluate were analyzed by MALDI-MS (see supplemental Fig. S1). The results revealed a specific binding of the glycans to the affinity matrix, thus clearly demonstrating that these oligosaccharides represented, in fact, cross-reacting species.

**Structural Characterization of Difucosylated Serologically Cross-reacting KLH Glycans**—Recovered major PA-oligosaccharide subfractions (see Fig. 6, TABLE TWO, and supplemental Table S1) were subjected to MALDI-MS/MS(LID) (tandem mass spectrometry after laser-induced dissociation), linkage analysis, chromium trioxide oxidation, chemical defucosylation by HF treatment, or digestion with exoglycosidases in conjunction with MALDI-MS. Selected fractions were further studied by MALDI-MS/MS(CID) (tandem mass spectrometry after collision-induced dissociation) and nano-LC-ESI-IT-MS/MS. The results revealed a number of structural parameters that were common to all glycans studied. Linkage analysis, for example, demonstrated that all of them comprised terminal fucose, terminal galactose, 3-substituted GalNAc, and 3,4-disubstituted GlcNAc residues (supplemental Table S1). Terminal mannose was not detectable. In agreement with previous studies (23) that demonstrated a partial conversion of 3-substituted GalNAc and 3,4-disubstituted GlcNAc into terminal GalNAc and 4-substituted GlcNAc upon chemical defucosylation of total KLH glycopeptides, these findings are consistent with the presence of a Fuc(1–3)GalNAc(1–4)[Fuc(1–3)]GlcNAc carbohydrate motif.

Glycan fractions comprising species with a pentose residue exhibited, in addition, terminal xylose and 2,3,6-trisubstituted mannose. The present xylose residue could be, therefore, assigned to C-2 of the central mannose of the pentasaccharide *N*-glycan core. With the exception of fraction 15-1 glycans, which expressed a 4,6-disubstituted GlcNAc residue, all oligosaccharides contained 4-substituted GlcNAc, which is assumed to originate from the PA-modified chitobiose cores of these molecules. Intriguingly, galactose was found exclusively in terminal positions. Whereas all glycan fractions exhibited a related pattern of 2,4- and 3,6-disubstituted mannose residues, differences could be observed with respect to the presence of 2,6-disubstituted, 2-substituted, or 6-substituted mannosyl residues, thus reflecting subtle structural differences (supplemental Table S1). Hence, monosubstituted mannose occurred only in low abundance in agreement with a highly branched architecture of most of the glycans.

Sequential exoglycosidase digestion with jack bean  $\beta$ -galactosidase and  $\alpha$ -mannosidase in combination with MALDI-MS revealed the release of one Gal and zero to two Man residues (supplemental Table S1). The finding of only one Gal being liberated is remarkable, because this monosaccharide represented the sole terminal sugar constituent apart from fucose and xylose and has been shown to be  $\beta$ -linked by chromium trioxide oxidation (data not shown). Possibly, efficient release of these moieties is impaired by sterical hindrance and/or the type of glycosidic linkages some of which might be resistant to the enzyme employed. Treatment with  $\alpha$ -galactosidase from green coffee beans, performed as a further control, did not result in any release of galactosyl residues.

The  $\alpha$ -anomeric configuration of fucose was verified by chromium trioxide oxidation as well as by  $\alpha$ -fucosidase treatment, although only one fucose was released by the enzyme in each case (supplemental Table S1). This finding is in agreement with earlier studies that demonstrated

TABLE TWO					
Analysis of KLH-derived cross-reacting PA-glycans by MALDI-MS/MS following LID or CID and by nano-ESI-IT-MS/MS					
Compositional species <sup>a</sup>	Mass <sup>b</sup> [M+H] <sup>+</sup> ([M+Na] <sup>+</sup> )	Glycan fraction	Diagnostic fragment ions obtained by		
			MALDI-MS/MS(LID) <sup>c</sup>	MALDI-MS/MS(CID) <sup>d</sup>	
H <sub>4</sub> N <sub>4</sub> F <sub>2</sub> PA	1849.8 (1872.9)	12-3	1151.4 (H <sub>4</sub> N <sub>2</sub> PA), 699.3 (N <sub>2</sub> F <sub>2</sub> ), 553.2 (N <sub>2</sub> F <sub>1</sub> ), 503.2 (N <sub>2</sub> PA), 350.1 (N <sub>1</sub> F <sub>1</sub> )	1173.4 (Y <sub>4α</sub> ), 1011.4 (Y <sub>3α</sub> ), 671.2 (B <sub>5</sub> Y <sub>4α</sub> ), 525.2 (Y <sub>2α</sub> ), 509.2 (B <sub>5</sub> Y <sub>3α</sub> = D-ion), 421.2 ( <sup>3,5</sup> A <sub>5</sub> )	689.2/671.2 (H <sub>4</sub> ), 527.2/509.2 (H <sub>3</sub> ), 467.2/437.2/407.2 (H <sub>3</sub> ring fragmentation)
H <sub>5</sub> N <sub>4</sub> F <sub>2</sub> PA	2011.8 (2034.9)	13-2		1335.5 (Y <sub>4α</sub> ), 1011.4 (Y <sub>3α</sub> ), 833.3 (B <sub>5</sub> Y <sub>4α</sub> ), 525.2 (Y <sub>2α</sub> ), 509.2 (B <sub>5</sub> Y <sub>3α</sub> = D-ion), 421.2 ( <sup>3,5</sup> A <sub>5</sub> ), 407.2 ( <sup>0,4</sup> A <sub>5</sub> )	
		14-1	1313.6 (H <sub>5</sub> N <sub>2</sub> PA), 699.2 (N <sub>2</sub> F <sub>2</sub> ), 553.1 (N <sub>2</sub> F <sub>1</sub> ), 503.3 (N <sub>2</sub> PA), 350.2 (N <sub>1</sub> F <sub>1</sub> )	1335.5 (Y <sub>4α</sub> ), 1173.4 (Y <sub>3α</sub> ), 833.3 (B <sub>5</sub> Y <sub>4α</sub> ), 671.2 (B <sub>5</sub> Y <sub>3α</sub> = D-ion), 583.2 ( <sup>3,5</sup> A <sub>5</sub> ), 569.2 ( <sup>0,3</sup> A <sub>5</sub> ), 525.2 (Y <sub>2α</sub> )	1335.5 (H <sub>5</sub> N <sub>2</sub> PA), 851.3/833.3 (H <sub>5</sub> ), 689.2/671.2 (H <sub>4</sub> ), 629.2/599.2/569.3 (H <sub>4</sub> ring fragmentation)
H <sub>5</sub> N <sub>4</sub> F <sub>2</sub> X <sub>1</sub> PA	2143.9 (2167.2)	12-3		ND <sup>e</sup>	ND
		13-1		ND	
		14-2	1444.9 (H <sub>5</sub> N <sub>2</sub> X <sub>1</sub> PA), 699.1 (N <sub>2</sub> F <sub>2</sub> ), 553.1 (N <sub>2</sub> F <sub>1</sub> ), 503.2 (N <sub>2</sub> PA), 350.1 (N <sub>1</sub> F <sub>1</sub> )	1467.4 (Y <sub>4α</sub> ), 965.3 (B <sub>5</sub> Y <sub>4α</sub> ), 803.3 (B <sub>5</sub> Y <sub>3α</sub> = D-ion), 569.2 ( <sup>0,4</sup> A <sub>5</sub> )	
		15-3		1467.4 (Y <sub>4α</sub> ), 965.3 (B <sub>5</sub> Y <sub>4α</sub> ), 641.2 (B <sub>5</sub> Y <sub>3α</sub> = D-ion), 421.2 ( <sup>3,5</sup> A <sub>5</sub> ), 407.2 ( <sup>0,4</sup> A <sub>5</sub> )	
H <sub>6</sub> N <sub>4</sub> F <sub>2</sub> PA	2173.9 (2197.2)	13-1		ND	ND
		15-1		ND	
		14-2, 15-2, 15-3	1475.6 (H <sub>6</sub> N <sub>2</sub> PA), 699.3 (N <sub>2</sub> F <sub>2</sub> ), 553.2 (N <sub>2</sub> F <sub>1</sub> ), 503.2 (N <sub>2</sub> PA), 350.1 (N <sub>1</sub> F <sub>1</sub> )	1896.7 (B <sub>6</sub> ), 1531.5 (B <sub>5</sub> ), 1385.5 (B <sub>5</sub> Y <sub>6α</sub> ), 1497.5 (Y <sub>4α</sub> ), 1173.4 (Y <sub>3α</sub> ), 833.3 (B <sub>5</sub> Y <sub>4α</sub> ), 715.3 ( <sup>1,5</sup> X <sub>2</sub> ), 687.3 (Y <sub>2</sub> ), 669.3 (Z <sub>2</sub> ), 509.2 (B <sub>5</sub> Y <sub>3α</sub> = D-ion), 421.2 ( <sup>3,5</sup> A <sub>5</sub> ), 407.2 ( <sup>0,4</sup> A <sub>5</sub> ), 388.1 (B <sub>6</sub> Y <sub>2</sub> ), 1896.7 (B <sub>6</sub> ), 1693.6 (B <sub>5</sub> ), 1497.5 (Y <sub>4α</sub> ), 1198.4 (B <sub>6</sub> Y <sub>4α</sub> ), 1173.4 (Y <sub>3α</sub> ), 995.3 (B <sub>5</sub> Y <sub>4α</sub> ), 671.2 (B <sub>5</sub> Y <sub>3α</sub> = D-ion), 583.2 ( <sup>3,5</sup> A <sub>5</sub> ), 569.2 ( <sup>0,4</sup> A <sub>5</sub> ), 553.2 ( <sup>1,5</sup> X <sub>2</sub> ), 525.2 (Y <sub>2α</sub> ), 507.2 (Z <sub>2α</sub> )	

<sup>a</sup> H<sub>1</sub> hexose; N<sub>1</sub> N'-acetylhexosamine; F<sub>1</sub> fucose; X<sub>1</sub> xylose; PA, pyridylamine residue.

<sup>b</sup> Pseudomolecular ions were determined with isotopic resolution ([M + H]<sup>+</sup>) or as average masses ([M + Na]<sup>+</sup>).

<sup>c</sup> Proton adducts.

<sup>d</sup> Monoisotopic sodium adducts.

ND, not done.

<sup>a</sup> H, hexose; N, N-acetylhexosamine; F, fucose; X, xylose; PA, pyridylamine residue.<sup>b</sup> Pseudomolecular ions were determined with isotopic resolution ([M + H]<sup>+</sup> or as average masses ([M + Na]<sup>+</sup>).<sup>c</sup> Proton adducts.<sup>d</sup> Monoisotopic sodium adducts.<sup>e</sup> ND, not done.

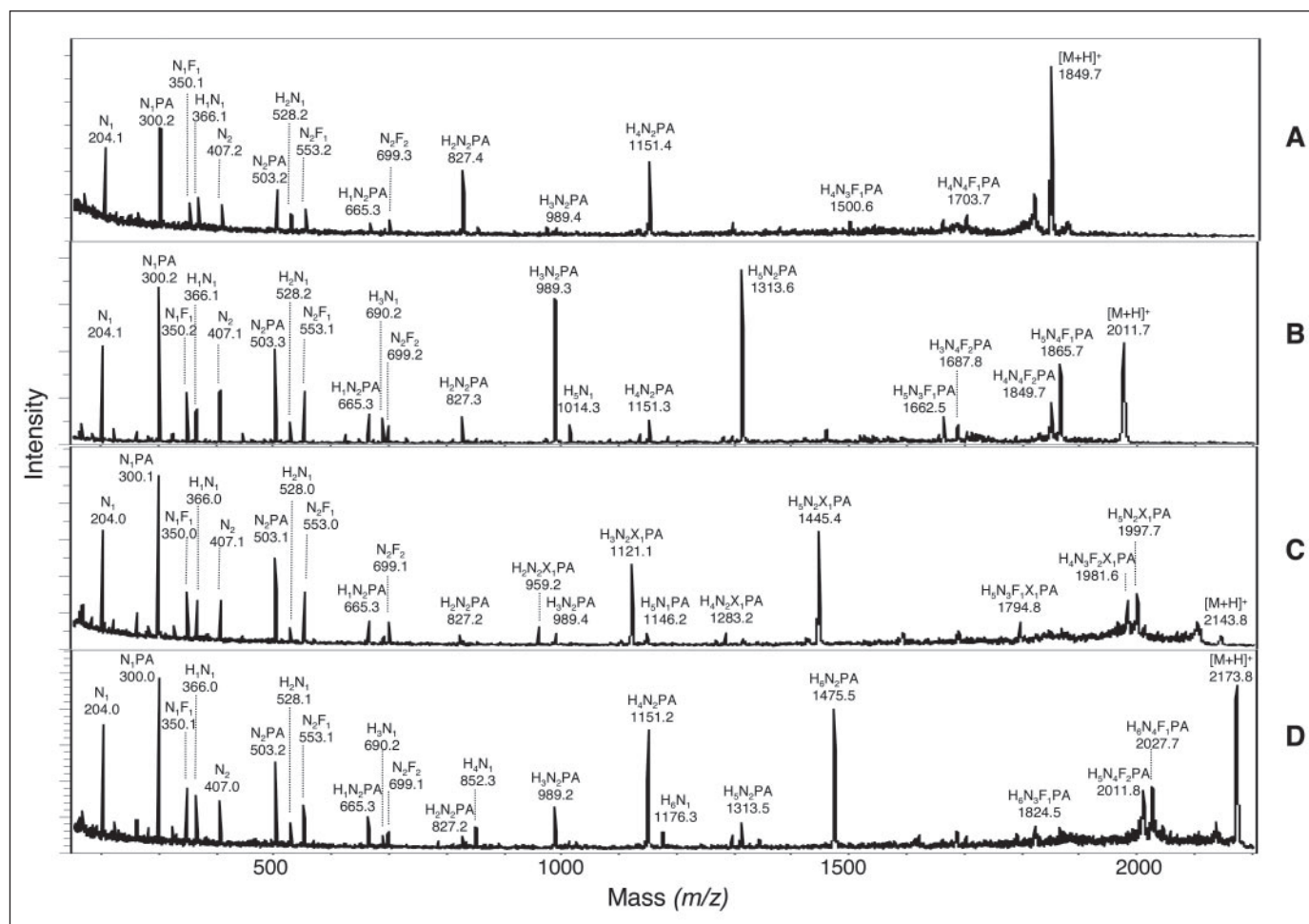


FIGURE 7. MALDI-MS/MS(LID) of individual PA-oligosaccharides. Protonated pseudomolecular ions  $[M+H]^+$  of the PA-glycan species Hex<sub>4</sub>HexNac<sub>4</sub>Fuc<sub>2</sub>PA (A), Hex<sub>5</sub>HexNac<sub>4</sub>Fuc<sub>2</sub>PA (B), Hex<sub>5</sub>HexNac<sub>4</sub>Fuc<sub>2</sub>Xyl<sub>1</sub>PA (C), and Hex<sub>6</sub>HexNac<sub>4</sub>Fuc<sub>2</sub>PA (D), present in fractions 12-3, 13-2, 15-3, or 15-2, respectively, were subjected to MALDI-MS/MS following laser-induced dissociation. Respective monosaccharide compositions are assigned to all relevant fragments. H, hexose; N, N-acetylhexosamine; F, fucose; X, xylose.

that one fucosyl residue may be released from Fuc( $\alpha$ 1-3)GalNac( $\beta$ 1-4)[Fuc( $\alpha$ 1-3)]GlcNac( $\beta$ 1-moieties by  $\alpha$ -fucosidase from bovine kidney, whereas none is liberated from GalNac( $\beta$ 1-4)[Fuc( $\alpha$ 1-3)]GlcNac( $\beta$ 1 units (38). Chemical defucosylation plus  $\beta$ -N-acetylhexosaminidase treatment resulting in the liberation of two fucoses and two HexNac residues prior to incubation with  $\beta$ -galactosidase and  $\alpha$ -mannosidase did not lead to an increased release of Gal or Man, thus ruling out a sterical hindrance of the latter enzymes by the Fuc( $\alpha$ 1-3)GalNac( $\beta$ 1-4)[Fuc( $\alpha$ 1-3)]GlcNac( $\beta$ 1-moiety.

**Analysis of Difucosylated Serologically Cross-reacting KLH Glycans by Mass Spectrometry**—MALDI-MS/MS(LID) analyses of the major Hex<sub>4-6</sub>HexNac<sub>4</sub>Fuc<sub>2</sub>Xyl<sub>0-1</sub> species obtained (Fig. 6) provided additional structural information. In each case resulting mass spectra revealed the preferential loss of a HexNac<sub>2</sub>Fuc<sub>2</sub> moiety as evidenced by B-type fragment ions with compositions of HexNac<sub>1</sub>, HexNac<sub>1</sub>Fuc<sub>1</sub>, HexNac<sub>2</sub>Fuc<sub>1</sub>, and HexNac<sub>2</sub>Fuc<sub>2</sub> leading to major Y-type fragments with compositions of Hex<sub>4-6</sub>HexNac<sub>2</sub>Xyl<sub>0-1</sub>PA (Fig. 7 and TABLE TWO). In addition, series of minor fragments were registered reflecting the sequential loss of four to six hexoses and one xylose, if present, as well as one HexNac residue yielding a final HexNacPA moiety. Hence, the obtained MALDI-MS/MS(LID) spectra confirmed unambiguously the presence of the aforementioned terminal difucosylated GalNac(1-4)GlcNac unit. In all cases, intense signals at  $m/z$  503 (HexNac<sub>2</sub>PA) were detected, whereas signals at  $m/z$  446 (HexNac<sub>1</sub>Fuc<sub>1</sub>PA) were not

registered. Therefore, it can be concluded that this set of cross-reactive glycans lacked core fucosylation. Isomeric compounds obtained, for example, in the case of Hex<sub>6</sub>HexNac<sub>4</sub>Fuc<sub>2</sub> species in fractions 15-1 to 15-3 (TABLE TWO) further revealed, in part, changes in fragment ion intensities that might reflect differences in structure (data not shown). Due to the lack of appropriate PA-oligosaccharide standards, however, this information could not be used for structural assignments.

To allocate the identified difucosylated GalNac(1-4)GlcNac unit within the glycan molecule, Hex<sub>4</sub>HexNac<sub>4</sub>Fuc<sub>2</sub>PA and Hex<sub>5</sub>HexNac<sub>4</sub>Fuc<sub>2</sub>PA species were subjected to nano-LC-ESI-IT-MS<sup>n</sup>. The results revealed again a preferential loss of the terminal HexNac<sub>2</sub>Fuc<sub>2</sub> unit in the MS<sup>2</sup> spectrum resulting in an Y<sub>4 $\alpha$</sub>  type of fragment ion (see, for example, Fig. 8 and TABLE TWO). Analysis of this fragment ion by an additional isolation and fragmentation cycle revealed in the corresponding MS<sup>3</sup> spectrum two pairs of ions (B<sub>5</sub>Y<sub>4 $\alpha$</sub> /C<sub>5</sub>Y<sub>4 $\alpha$</sub>  and B<sub>5</sub>Y<sub>3 $\alpha$</sub> /C<sub>5</sub>Y<sub>3 $\alpha$</sub> ). Intriguingly, C<sub>5</sub>Y<sub>4 $\alpha$</sub>  ions obtained from precursors with four (Hex<sub>4</sub>HexNac<sub>4</sub>Fuc<sub>2</sub>PA, not shown) or five (Hex<sub>5</sub>HexNac<sub>4</sub>Fuc<sub>2</sub>PA; Fig. 8B) hexose units did not yield further ring fragmentation. In agreement with previous studies (39), it can, therefore, be concluded that the reducing hexose is still substituted at C3 in this fragment. In contrast, related C<sub>5</sub>Y<sub>3 $\alpha$</sub>  ions, comprising three (Hex<sub>4</sub>HexNac<sub>4</sub>Fuc<sub>2</sub>PA) or four (Hex<sub>5</sub>HexNac<sub>4</sub>Fuc<sub>2</sub>PA) hexose units, allowed further ring fragmentation in accordance with a C6 substitution of the reducing hexose. From these results it can be concluded that the difucosylated GalNac(1-

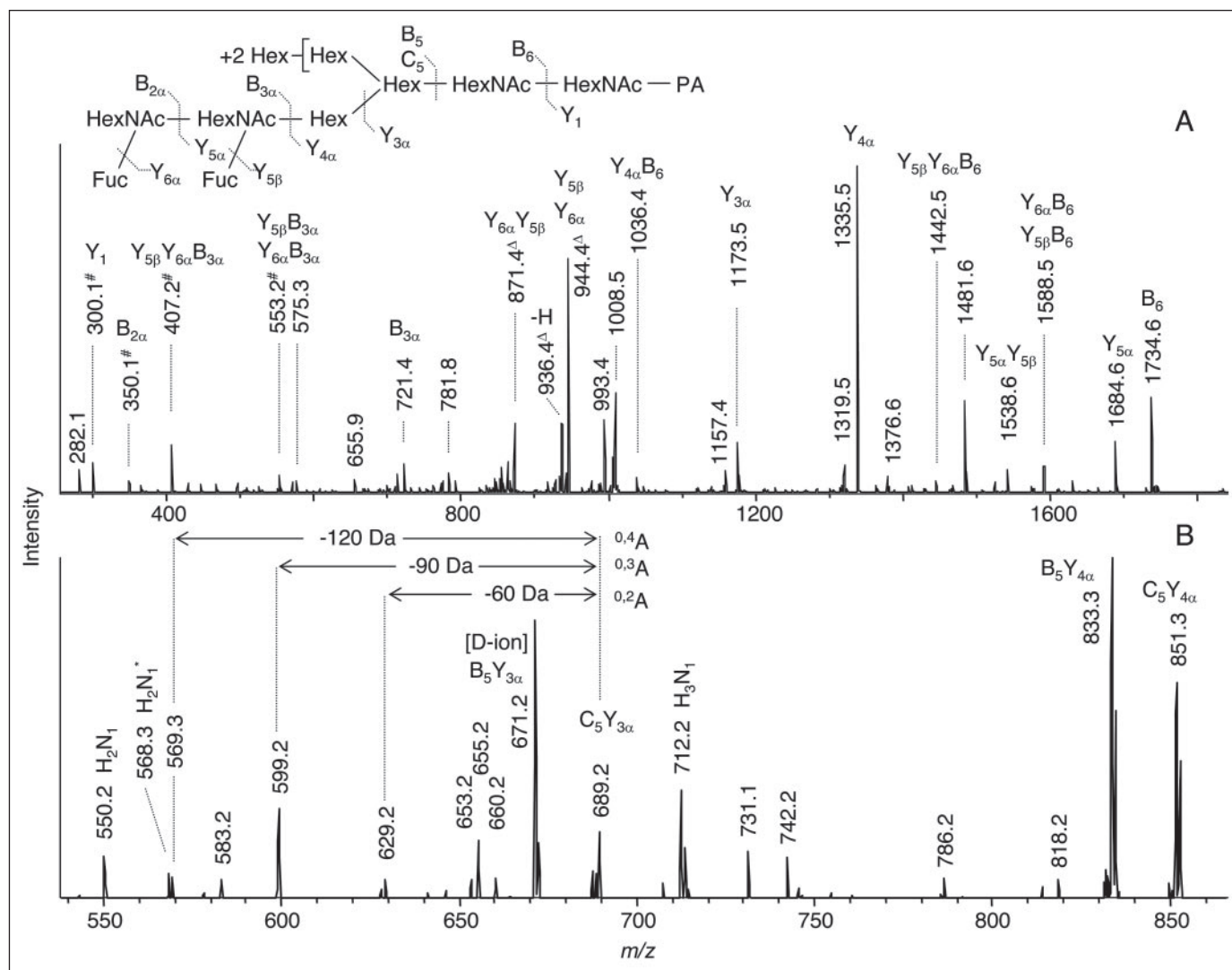


FIGURE 8. **Analysis of Hex<sub>5</sub>HexNac<sub>4</sub>Fuc<sub>3</sub>PA species by normal phase-nano-LC-ESI-IT-MS/MS.** A, MS/MS spectrum of  $m/z$  1017.9 ( $[M+H+Na]^{2+}$ ). Besides sodium adducts, also proton adducts (#) and double-charged fragments ( $\Delta$ ) arising from neutral loss were observed. -H, loss of a hexose unit. B, fragment ion analysis of the species at  $m/z$  1335.5 in the MS/MS spectrum after an additional ion isolation/fragmentation cycle. Sodium adducts ( $[M+Na]^+$ ) were registered. Fragments are assigned according to the nomenclature of Domon and Costello (61). H, hexose; N, N-acetylhexosamine. \*, C-type ion.

4)GlcNAc unit is attached to the 3-linked mannose of the pentasaccharide core of the oligosaccharide. Additional analyses by off-line nano-ESI-MS/MS consistently confirmed that (a) the innermost GlcNAc of these glycans is not fucosylated and (b) outer HexNAc residues carried only one fucosyl residue each (data not shown).

For further structural assignment difucosylated cross-reacting glycans were analyzed by MALDI-MS/MS employing high energy CID. Analysis of Hex<sub>4</sub>HexNac<sub>4</sub>Fuc<sub>2</sub>PA species (fraction 12-3) led to Y<sub>4α</sub> (*m/z* 1173.4), Y<sub>3α</sub> (*m/z* 1011.4), B<sub>5</sub>Y<sub>4α</sub> (*m/z* 671.2) as well as the so-called “D-ion” B<sub>5</sub>Y<sub>3α</sub> (*m/z* 509.2) comprising three hexose units (see TABLE TWO and supplemental Fig. S2A). Only the D-ion led to <sup>3,5</sup>A<sub>5</sub> (*m/z* 421.2) and <sup>0,4</sup>A<sub>5</sub> (*m/z* 407.2) fragmentation due to ring cleavage of the core mannose (40, 41), thus demonstrating that this mannose carried two additional hexose moieties linked to its C6 position (*cf.* TABLE ONE). This finding is corroborated by the observed Y<sub>4α</sub> and Y<sub>3α</sub> ions, which verified that the 3-linked antenna comprised only one hexose residue. Furthermore, evidence for an unsubstituted chitobiose core has been provided by an Y<sub>2α</sub> fragment ion (*m/z* 525.2) with a composition of HexNac<sub>3</sub>PA. In conclusion, MALDI-MS/MS(CID) data are in perfect

agreement with the assignment made by ESI-ion trap-MS<sup>n</sup> described above.

By the same line of reasoning Hex<sub>5</sub>HexNac<sub>4</sub>Fuc<sub>2</sub>PA species obtained in fractions **13-2** and **14-1** (Fig. 6) were shown to represent two different structural isomers (TABLE ONE) carrying either two (fraction **13-2** glycans) or three (**14-1**) hexose residues at C6 of the branching mannose as evidenced by the respective D-ions and corresponding <sup>3,5</sup>A<sub>5</sub> and <sup>0,4</sup>A<sub>5</sub> ring fragmentation (TABLE TWO and supplemental Fig. S2, *B* and *C*). The latter structural isomer has been also identified by ESI-ion trap-MS<sup>n</sup>. The observed Y<sub>2α</sub> fragment ion (HexNac<sub>2</sub>PA) verified again an unsubstituted chitobiose core of these oligosaccharides.

Hex<sub>6</sub>HexNAc<sub>4</sub>Fuc<sub>2</sub>PA species obtained in fractions **15-1** (Fig. 6) represented a novel type of *N*-glycan carrying a galactosyl residue linked to C6 of the penultimate GlcNAc of the chitobiose core. This unusual structural feature could be verified by methylation analysis (see supplemental Table S1) and, in particular, by MALDI- MS/MS(CID) due to (a) the observed mass difference between the registered B<sub>6</sub> (*m/z* 1896.7) and B<sub>5</sub> (*m/z* 1531.5) fragment ions amounting 365 mass units in agreement with a loss of a Hex<sub>1</sub>HexNAc<sub>1</sub> unit (Fig. 9A and TABLE TWO), (b)



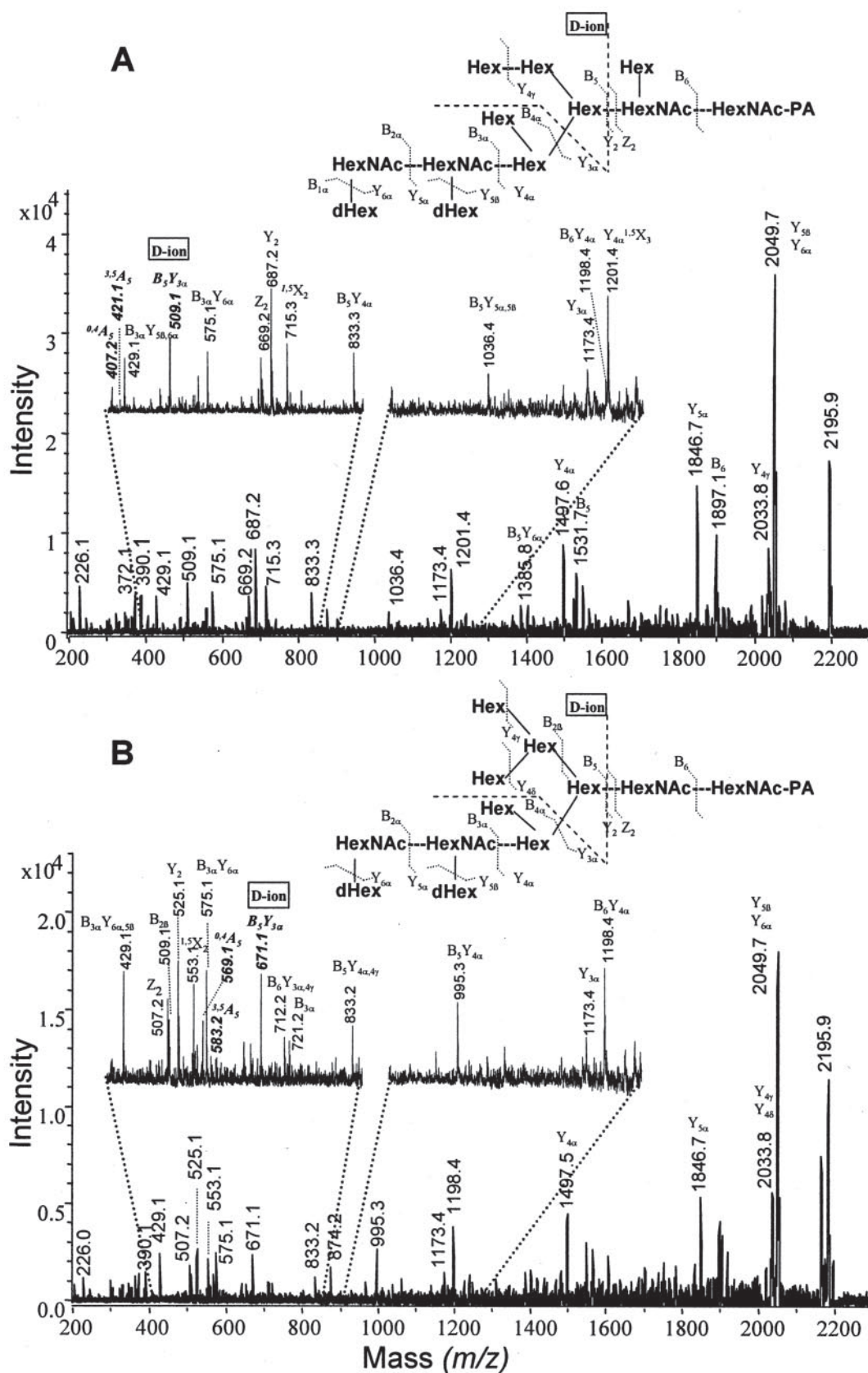


FIGURE 9. Analysis of isomeric Hex<sub>6</sub>HexNAc<sub>4</sub>Fuc<sub>2</sub>PA species by MALDI-MS/MS(CID). Sodiated pseudomolecular ions ([M+Na]<sup>+</sup>) of Hex<sub>6</sub>HexNAc<sub>4</sub>Fuc<sub>2</sub>PA species obtained in fractions 15-1 (A) and 15-3 (B) were subjected to MALDI-MS/MS after high energy collision-induced dissociation. Fragment ions are assigned according to Domon and Costello (61). Diagnostically relevant D-ions and ions resulting from A-type ring fragmentation are printed in *italics* and **bold**.

TABLE THREE

## Analysis of KLH-derived trifucosylated cross-reacting PA-glycans by MALDI-MS/MS(LID)

Compositional species <sup>a</sup>	Mass <sup>b</sup> [M + H] <sup>+</sup> ([M + Na] <sup>+</sup> )	Glycan fraction	Diagnostic fragment ions obtained by MALDI-MS/MS(LID) <sup>c</sup>
H <sub>3</sub> N <sub>4</sub> F <sub>3</sub> PA	1833.9 (1856.7)	12 (50 mM Fuc eluate)	1135.3 (H <sub>3</sub> N <sub>2</sub> F <sub>1</sub> PA), 811.3 (H <sub>1</sub> N <sub>2</sub> F <sub>1</sub> PA), 699.3 (N <sub>2</sub> F <sub>2</sub> ), 649.3 (N <sub>2</sub> F <sub>1</sub> PA), 553.2 (N <sub>2</sub> F <sub>1</sub> ), 446.3 (N <sub>1</sub> F <sub>1</sub> PA), 350.1 (N <sub>1</sub> F <sub>1</sub> )
H <sub>4</sub> N <sub>4</sub> F <sub>3</sub> PA	1995.9 (2018.9)	13 (50 mM Fuc eluate)	1297.4 (H <sub>4</sub> N <sub>2</sub> F <sub>1</sub> PA), 811.3 (H <sub>1</sub> N <sub>2</sub> F <sub>1</sub> PA), 699.3 (N <sub>2</sub> F <sub>2</sub> ), 649.3 (N <sub>2</sub> F <sub>1</sub> PA), 553.2 (N <sub>2</sub> F <sub>1</sub> ), 446.2 (N <sub>1</sub> F <sub>1</sub> PA), 350.1 (N <sub>1</sub> F <sub>1</sub> )
H <sub>5</sub> N <sub>4</sub> F <sub>3</sub> PA	2157.8 (2181.3)	14 (50 mM Fuc eluate)	1459.5 (H <sub>5</sub> N <sub>2</sub> F <sub>1</sub> PA), 811.3 (H <sub>1</sub> N <sub>2</sub> F <sub>1</sub> PA), 699.3 (N <sub>2</sub> F <sub>2</sub> ), 649.3 (N <sub>2</sub> F <sub>1</sub> PA), 553.3 (N <sub>2</sub> F <sub>1</sub> ), 446.2 (N <sub>1</sub> F <sub>1</sub> PA), 350.0 (N <sub>1</sub> F <sub>1</sub> )
H <sub>5</sub> N <sub>4</sub> F <sub>3</sub> XPA	2290.0	Immunoaffinity eluate	1591.7 (H <sub>5</sub> N <sub>2</sub> F <sub>1</sub> X <sub>1</sub> PA), 811.3 (H <sub>1</sub> N <sub>2</sub> F <sub>1</sub> PA), 699.3 (N <sub>2</sub> F <sub>2</sub> ), 649.3 (N <sub>2</sub> F <sub>1</sub> PA), 608.3 (H <sub>1</sub> N <sub>1</sub> F <sub>1</sub> PA), 553.1 (N <sub>2</sub> F <sub>1</sub> ), 446.1 (N <sub>1</sub> F <sub>1</sub> PA), 350.0 (N <sub>1</sub> F <sub>1</sub> )
H <sub>6</sub> N <sub>4</sub> F <sub>3</sub> PA	2320.0	Immunoaffinity eluate	2033.7 (H <sub>5</sub> N <sub>4</sub> F <sub>2</sub> PA), 1621.6 (H <sub>6</sub> N <sub>2</sub> F <sub>1</sub> PA), 811.3 (H <sub>1</sub> N <sub>2</sub> F <sub>1</sub> PA), 699.3 (N <sub>2</sub> F <sub>2</sub> ), 649.3 (N <sub>2</sub> F <sub>1</sub> PA), 608.1 (H <sub>1</sub> N <sub>1</sub> F <sub>1</sub> PA), 553.2 (N <sub>2</sub> F <sub>1</sub> ), 446.1 (N <sub>1</sub> F <sub>1</sub> PA), 350.0 (N <sub>1</sub> F <sub>1</sub> )

<sup>a</sup> H, hexose; N, *N*-acetylhexosamine; F, fucose; X, xylose; PA, pyridylamine residue.<sup>b</sup> Pseudomolecular ions were determined with isotopic resolution ([M + H]<sup>+</sup>) or as average masses ([M + Na]<sup>+</sup>).<sup>c</sup> Proton adducts.

the presence of a B<sub>5</sub>Y<sub>6α</sub> ion at *m/z* 1385.5 (Hex<sub>5</sub>HexNac<sub>2</sub>Fuc<sub>1</sub>), (c) the diagnostically relevant Y<sub>2</sub> fragment ion at *m/z* 687.3 (Hex<sub>1</sub>HexNac<sub>2</sub>PA) together with corresponding <sup>1,5</sup>X<sub>2</sub> (*m/z* 715.3) and Z<sub>2</sub> ions (*m/z* 669.3), (d) a B<sub>6</sub>Y<sub>2</sub> fragment of *m/z* 388.1 (Hex<sub>1</sub>HexNac<sub>1</sub>), and (e) the lack of a B<sub>5</sub>Y<sub>4α</sub> fragment at *m/z* 995.3 (Hex<sub>6</sub>). Instead, a B<sub>5</sub>Y<sub>4α</sub> fragment at *m/z* 833.3 (Hex<sub>5</sub>) as well as a B<sub>5</sub>Y<sub>3α</sub> fragment (D-ion) at *m/z* 509.2 (Hex<sub>3</sub>) were registered together with a corresponding <sup>3,5</sup>A<sub>5</sub> (*m/z* 421.2) and <sup>0,4</sup>A<sub>5</sub> (*m/z* 407.2) ring fragmentation. In addition, the mass difference between the Y<sub>4α</sub> (1497.5; Hex<sub>6</sub>HexNac<sub>2</sub>PA) and the Y<sub>3α</sub> fragment (1173.4; Hex<sub>4</sub>HexNac<sub>2</sub>PA) corresponded to two hexose units. Altogether, the obtained mass spectrum clearly demonstrated that this particular isomer carried two hexoses at C6 of the branching mannose, one hexose bound to the 3-linked mannose of the pentasaccharide core, and one hexose attached to the chitobiose unit (TABLE ONE).

In contrast to the fraction 15-1 Hex<sub>6</sub>HexNac<sub>4</sub>Fuc<sub>2</sub>PA species discussed before, similarly sized glycans obtained in fraction 15-3 (Fig. 6) led to B<sub>6</sub> (*m/z* 1896.7), B<sub>5</sub> (*m/z* 1693.6), Y<sub>2</sub> (*m/z* 525.2), Z<sub>2</sub> (*m/z* 507.2), and <sup>1,5</sup>X<sub>2</sub> (*m/z* 553.2) fragment ions, which clearly verified an unsubstituted chitobiose unit (Fig. 9B and TABLE TWO). Furthermore, a B<sub>5</sub>Y<sub>4α</sub> ion was detected at *m/z* 995.3 (Hex<sub>6</sub>) demonstrating that the six hexose residues were linked together. The corresponding D-ion (B<sub>5</sub>Y<sub>3α</sub>, *m/z* 671.2) comprised four hexoses and led to the expected <sup>3,5</sup>A<sub>5</sub> (*m/z* 583.2) and <sup>0,4</sup>A<sub>5</sub> (*m/z* 569.2) ring fragmentation. Hence, it can be concluded that these glycans carried three hexoses at C6 of the branching mannose and one hexose bound to the 3-linked mannose of the pentasaccharide core.

Hex<sub>6</sub>HexNac<sub>4</sub>Fuc<sub>2</sub>PA species obtained in fraction 14-2 furnished similar results as fraction 15-3 compounds. Because both glycans exhibited closely related retention times in reversed-phase HPLC (Fig. 6), it is assumed that they represent the same type of oligosaccharide species probably as a result of incomplete separation during size fractionation (Fig. 4A). In contrast, fraction 15-2 Hex<sub>6</sub>HexNac<sub>4</sub>Fuc<sub>2</sub>PA glycans clearly differed from fraction 15-1 and 15-3 oligosaccharides by their retention times in reverse-phase HPLC, but led to similar MALDI-MS/MS(CID) data with regard to the observed D-ion and subsequent ring fragmentation (TABLE TWO and supplemental Fig. S2F). Although comprising different structural isomers, fraction 15-2 and 15-3 glycans could, therefore, not be discriminated by this technique.

MALDI-MS/MS(CID) data of the Hex<sub>5</sub>HexNac<sub>4</sub>Fuc<sub>2</sub>Xyl<sub>1</sub>PA species obtained in fractions 14-2 and 15-3 were in full agreement with the above assignments. In both cases, B<sub>5</sub>Y<sub>4α</sub> fragment ions with *m/z* 965.3 were detected reflecting a composition of Hex<sub>5</sub>Xyl<sub>1</sub>. Corresponding D-ions (B<sub>5</sub>Y<sub>3α</sub>) with *m/z* 803.3 (Hex<sub>4</sub>Xyl<sub>1</sub>) or *m/z* 641.2 (Hex<sub>3</sub>Xyl<sub>1</sub>)

together with the respective <sup>3,5</sup>A<sub>5</sub> and <sup>0,4</sup>A<sub>5</sub> ring fragmentations were recovered in the case of fraction 14-2 and 15-3 glycans, respectively (TABLE TWO and supplemental Figs. S2, D and E). This finding corroborates the assignment made on the basis of methylation results (see supplemental Table S1) that xylose is linked to the central mannose of the pentasaccharide core. Based on these data, it could be concluded that these glycans represented the xylosylated variants of the Hex<sub>5</sub>HexNac<sub>4</sub>Fuc<sub>2</sub>PA isomers discussed above. Respective glycans obtained in fractions 12-3 and 13-1 could not be analyzed due to low amounts (30).

**Analysis of Trifucosylated Serologically Cross-reacting KLH Glycans—**Due to small amounts, trifucosylated cross-reactive glycans (Fig. 3) were only analyzed by MALDI-MS/MS(LID) (TABLE THREE and Fig. 10). In this context, it turned out, however, that the applied mass spectrometric techniques required in most cases a preceding fractionation of the sugar chains: when starting from the total mixture of cross-reacting glycans (Fig. 3) successful and efficient mass spectrometric isolation of the respective precursor ions was often impaired by the small mass differences between related compositional species, thus preventing the isolation of pure parent ions. In the case of Hex<sub>3</sub>HexNac<sub>4</sub>Fuc<sub>3</sub>PA, Hex<sub>4</sub>HexNac<sub>4</sub>Fuc<sub>3</sub>PA, and Hex<sub>5</sub>HexNac<sub>4</sub>Fuc<sub>3</sub>PA species recovered after lectin (AAL) affinity separation of aminophase HPLC fractions 12, 13, and 14 (Fig. 4) in the 50 mM Fuc eluates (Fig. 5) again B-type fragment ions were detected reflecting the preferential loss of a non-reducing difucosylated GalNac(1–4)GlcNAc unit (see signals at *m/z* 699.3 [HexNac<sub>2</sub>Fuc<sub>2</sub>], 553.2 [HexNac<sub>2</sub>Fuc<sub>1</sub>], and 350.1 [HexNac<sub>1</sub>Fuc<sub>1</sub>] in Fig. 10 and TABLE THREE). In addition, Y<sub>1</sub> and Y<sub>2</sub> fragment ions with *m/z* 446.3 (HexNac<sub>1</sub>Fuc<sub>1</sub>PA) and *m/z* 649.3 (HexNac<sub>2</sub>Fuc<sub>1</sub>PA) as well as fragments with *m/z* 811.3 (Hex<sub>1</sub>HexNac<sub>2</sub>Fuc<sub>1</sub>PA) were registered, thus verifying an additional fucosylation of the molecules at the innermost GlcNAc residue of their chitobiose core (Fig. 10A). The fragment ion spectra of Hex<sub>5</sub>HexNac<sub>4</sub>Fuc<sub>3</sub>Xyl<sub>1</sub>PA and Hex<sub>6</sub>HexNac<sub>4</sub>Fuc<sub>3</sub>PA species were generated directly from the total immunoaffinity eluate (Fig. 3). Intriguingly, both of them furnished in addition to the Y-type fragment ions with *m/z* 446.1, *m/z* 649.3, and *m/z* 811.3 a signal at *m/z* 608 corresponding to a fragment composition of Hex<sub>1</sub>HexNac<sub>4</sub>Fuc<sub>1</sub>PA (Fig. 10B). This finding is in agreement with earlier studies that demonstrated that the core-linked fucosyl residues of KLH-glycans may be, in part, further capped by galactosyl residues (21). Based on the sensitivity of the trifucosylated components toward PNGase F (42), the core fucose can be assigned to C6 of the innermost GlcNAc.

**Structural Conclusions—**Obtained analytical data allowed a number of important structural conclusions regarding the architecture of KLH N-glycans cross-reacting with *S. mansoni* glycoconjugates (see TABLE

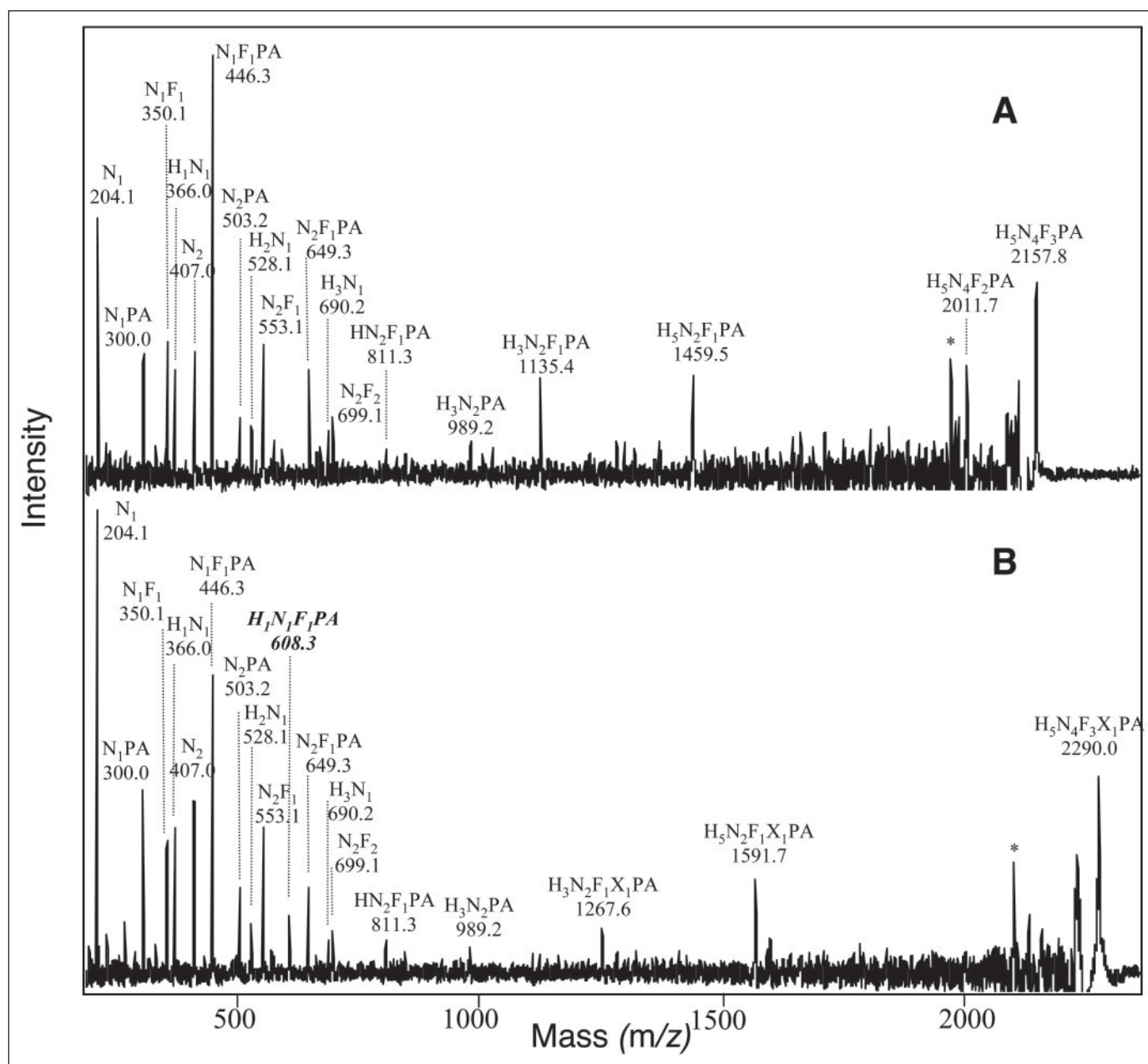


FIGURE 10. **Analysis of trifucosylated cross-reacting glycans by MALDI-MS/MS(LID).** Protonated pseudomolecular ions  $[M+H]^+$  of the PA-glycan species Hex<sub>5</sub>HexNAc<sub>4</sub>Fuc<sub>3</sub>PA (A) and Hex<sub>5</sub>HexNAc<sub>4</sub>Fuc<sub>3</sub>Xyl<sub>1</sub>PA (B), present in fraction 14 (50 mM Fuc eluate; Fig. 5G) or the immunoaffinity eluate (Fig. 3), respectively, were subjected to MALDI-MS/MS following laser-induced dissociation. Monosaccharide compositions of fragments are assigned. The diagnostically relevant fragment demonstrating the partial presence of a substituted core fucose in B is printed in *italics* and **bold**. Signals marked by asterisks reflect fragments produced by cleavage of the linkage between C-2 and C-3 of the pyridylaminated GlcNAc ( $-178.1$  Da). H, hexose; N, N-acetylhexosamine; F, fucose; X, xylose.

ONE). In agreement with previous data (23) the results unambiguously verified the presence of a terminal Fuc( $\alpha 1-3$ )GalNAc( $\beta 1-4$ )[Fuc( $\alpha 1-3$ )]GlcNAc( $\beta 1$ -unit, which could be assigned to the 3-linked mannosyl residue of the common pentasaccharide core by nano-LC-ESI-ion trap-MS<sup>n</sup> and MALDI-MS/MS(CID). Hence, all analyzed cross-reacting glycans comprised as a general feature a Man<sub>3</sub>GlcNAc<sub>2</sub>-pentasaccharide core the 3-linked mannose of which was further substituted at C2 by a Fuc( $\alpha 1-3$ )GalNAc( $\beta 1-4$ )[Fuc( $\alpha 1-3$ )]GlcNAc( $\beta 1$ -unit. This basic structure can be further decorated by xylose linked to C2 of the central mannose, a fucosyl residue at C6 of the innermost GlcNAc, and additional hexoses. Because (a) terminal hexose residues were found to represent exclusively Gal and (b) mannose units were mostly disubstituted, the structural heterogeneity of the studied glycans could be attributed to

different substitution patterns of the pentasaccharide core by a varying number of galactosyl residues. Three different types of structural variants could be identified: (a) Glycans in which additional Gal residues were exclusively bound to the 6-linked mannose (isomer I), (b) oligosaccharides in which one galactose was also attached to the 3-linked Man (isomer II), and (c) isomer II species exhibiting in addition a galactosyl residue at the penultimate GlcNAc residue of the chitobiose unit (isomer III). Hex<sub>4</sub>HexNAc<sub>4</sub>Fuc<sub>2</sub>PA species represented exclusively isomer I (TABLE ONE). Because 2-substituted Man was the sole monosubstituted mannosyl residue identified by linkage analysis of this fraction, the additional Gal residue may be assigned to C2 of the 6-linked mannose (TABLE ONE). Hex<sub>5</sub>HexNAc<sub>4</sub>Fuc<sub>2</sub>PA and Hex<sub>5</sub>HexNAc<sub>4</sub>Fuc<sub>2</sub>Xyl<sub>1</sub>PA species reflected both isomer I as well as isomer II compounds. Because the



corresponding glycan fractions studied by linkage analyses often represented mixtures of different compounds, a heterogeneous substitution pattern of the involved mannosyl residues was obtained. Therefore, allocation of terminal Gal units remained mostly ambiguous (TABLE ONE). In the case of fraction 15-1-derived Hex<sub>6</sub>HexNAc<sub>4</sub>Fuc<sub>2</sub>PA species, however, mass spectrometric analyses allowed in conjunction with linkage data a precise assignment of all additional Gal residues present (TABLE ONE). The proposed structure is further corroborated by the results obtained by sequential exoglycosidase treatment revealing the release of one  $\beta$ -linked galactose and one  $\alpha$ -linked mannosyl residue (see supplemental Table S1). Hence, these glycans represent a novel type of *N*-glycans comprising an unusual substitution of the chitobiose unit by an additional Gal residue. Remaining Hex<sub>6</sub>HexNAc<sub>4</sub>Fuc<sub>2</sub>PA species obtained in fraction 15-2 and 15-3 represented exclusively the isomer II type of glycans. Based on linkage data (*i.e.* occurrence of 6-substituted mannose as well as 2,4- and 3,6-disubstituted mannosyl residues) and exoglycosidase results (release of one  $\beta$ -linked galactose and two  $\alpha$ -linked mannosyl residues) fraction 15-2 glycans are concluded to exhibit a linear trisaccharide unit at C6 of the central mannose of the pentasaccharide core. In contrast, fraction 15-3 species comprised exclusively 2,4-, 2,6-, or 3,6-disubstituted mannose. Exoglycosidase treatment led to the release of one  $\beta$ -linked galactose, whereas subsequent liberation of mannosyl residues could not be achieved. Therefore, a highly branched structure can be proposed in this case, the outer galactose residues of which, however, could not be unambiguously assigned (TABLE ONE). In conclusion, this study provides for the first time a detailed characterization of the KLH *N*-glycans responsible for the known cross-reactivity with *S. mansoni*.

## DISCUSSION

The aim of this study was the characterization of glycans from keyhole limpet hemocyanin (KLH) sharing serologically cross-reacting carbohydrate motifs with glycoconjugates from *S. mansoni*. To this end oligosaccharides of KLH were released by hydrazinolysis or PNGase F and tagged with 2-aminopyridine. Cross-reacting glycans were identified by immunoaffinity chromatography using immobilized polyclonal antibodies directed against soluble egg antigens of *S. mansoni*. Respective oligosaccharides were isolated by sequential aminophase HPLC, lectin affinity chromatography, and reverse-phase HPLC and characterized in particular by different mass spectrometric techniques as well as linkage analysis and exoglycosidase treatment. The results revealed that all cross-reacting species represent novel types of *N*-glycans (*cf.* corresponding structures in TABLE ONE) all of which comprise a terminal Fuc( $\alpha$ 1-3)GalNAc( $\beta$ 1-4)[Fuc( $\alpha$ 1-3)]GlcNAc( $\beta$ 1-epitope, which has been reported to occur in glycosphingolipids and glycoprotein glycans from *S. mansoni* (38, 43–45). This finding is in agreement with recent observations demonstrating that the interaction of glycolipids from different *S. mansoni* life-cycle stages with monoclonal antibodies recognizing Fuc( $\alpha$ 1-3)GalNAc( $\beta$ 1-4)GlcNAc- and/or Fuc( $\alpha$ 1-3)-GalNAc( $\beta$ 1-4)[Fuc( $\alpha$ 1-3)]GlcNAc-epitopes could be inhibited by KLH, whereas binding of antibodies directed against Gal( $\beta$ 1-4)-[Fuc( $\alpha$ 1-3)]GlcNAc- (Lewis X), GalNAc( $\beta$ 1-4)[Fuc( $\alpha$ 1-3)]GlcNAc, and GalNAc( $\beta$ 1-4)[Fuc( $\alpha$ 1-2)Fuc( $\alpha$ 1-3)]GlcNAc units was not impaired (46).

Analysis of the carbohydrate structure of KLH proved to be an extremely difficult task due to the vast microheterogeneity of its glycans resulting in the expression of a great variety of different isomeric and/or isobaric structures. This feature has been already recognized in the case of the high mannose-type glycans and paucimannosidic sugar chains, which represent major carbohydrate substituents of KLH (20). Our present study shows that structural microheterogeneity is even more

pronounced in the case of the numerous minor constituents present. According to our experience, the only way to analyze these glycans is to focus on defined structural or biological features expressed by distinct subpopulations of KLH sugar chains. In this study we have, therefore, concentrated exclusively on glycans serologically cross-reacting with *S. mansoni* glycoconjugates. In this context it should be emphasized, however, that the structural assignments made would not have been possible without prior separation of these oligosaccharides by different HPLC methods. Without fractionation, MALDI-MS/MS (LID or CID) analyses showed in most cases contaminations by neighboring signals due to an inefficient isolation of pure parent ions. Furthermore, the quality of CID spectra is known to strongly depend on the complexity of the sample (30).

We have demonstrated previously (23) that a Fuc( $\alpha$ 1-3)GalNAc motif is implicated in the cross-reactivity of *S. mansoni* infection sera with KLH. In that study, however, only an unfractionated mixture of total KLH glycopeptides has been employed. In the present contribution, the relevant carbohydrate chains have been isolated, individually characterized, and identified as *N*-glycans. Due to the structural heterogeneity mentioned above, however, it was not possible to obtain homogeneous oligosaccharide fractions, although a three-dimensional fractionation scheme has been employed. Furthermore, the oligosaccharides of interest represented minor compounds and could be isolated only in small amounts. As judged from the peak intensities of the MALDI spectra, cross-reacting difucosylated glycans, comprising six compositional species, represented  $\sim$ 3% of total PNGase F-released carbohydrates, whereas trifucosylated oligosaccharides, encompassing nine different species, comprise only 1.5%. Therefore, it was not possible to fully establish the structures for all cross-reacting oligosaccharides under study. The common feature of these glycans, however, could be unambiguously identified as being composed of a Man<sub>3</sub>GlcNAc<sub>2</sub> pentasaccharide core the 3-linked mannose of which is further substituted at C2 by the Fuc( $\alpha$ 1-3)GalNAc( $\beta$ 1-4)[Fuc( $\alpha$ 1-3)]GlcNAc( $\beta$ 1-moiety. As evidenced by minor cross-reacting species with compositions of Hex<sub>2</sub>HexNAc<sub>4</sub>Fuc<sub>3</sub> (Fig. 3) truncated variants lacking the 6-linked Man might also occur in small amounts. In most cases, however, the pentasaccharide core is further decorated by one to three galactosyl residues. In this context, a novel type of *N*-glycan could be identified carrying galactose at C6 of the penultimate GlcNAc residue of the chitobiose unit. Further modifications of the core structure include the substitution of the central mannose at C2 by xylose and/or the attachment of an additional Fuc residue to C6 of the innermost GlcNAc, which may be, in turn, further substituted by a galactosyl residue in agreement with previous data (21). In conclusion, the cross-reacting KLH carbohydrates represent a distinct class of glycoprotein-glycans.

In previous studies, galactosyl residues have been shown to occur in different positions in KLH glycans, including Gal( $\beta$ 1-6)Man, Gal( $\beta$ 1-4)GlcNAc, Gal( $\beta$ 1-3)GlcNAc, and GlcNAc( $\beta$ 1-2)[Gal( $\beta$ 1-6)]Man (20) as well as Gal( $\beta$ 1-4)Gal and Gal( $\beta$ 1-4)Fuc linkages (21). In the present contribution, linkage analysis data suggest that galactose may also occur in Gal( $\beta$ 1-2)Man and Gal( $\beta$ 1-4)Man linkages, leading, in part, to 2,4-disubstituted and further 2,6-disubstituted mannosyl residues. Because these analyses were mostly performed on mixtures of glycans or different isomers, assignment of the exact linkage positions of galactosyl residues remains ambiguous in most cases. Likewise, recorded MALDI-MS/MS spectra did not yield sufficient ring cleavage ions to substantiate defined linkage positions of the galactose units. Possibly due to the small amounts of glycans available for these studies, MS/MS spectra obtained under CID conditions were dominated by glycosidic B-/Y-ions and displayed only less intense cross-ring cleavage



ions (30). It has to be pointed out, however, that the present galactosyl residues are obviously not crucial for antibody binding.

Using peanut agglutinin and anti-Gal( $\beta$ 1–3)GalNAc IgM antibodies, Wirguin *et al.* (8) demonstrated that KLH contains Gal( $\beta$ 1–3)GalNAc-bearing oligosaccharides. Furthermore, immunization with KLH-induced antibodies cross-reacting with the Thomson-Friedenreich (T) antigen. This finding has been later interpreted as an indication of O-glycosylation of KLH (47). To our knowledge, however, O-glycans have neither been isolated from KLH nor characterized yet. Insofar this point is important, because it has been suggested that these Gal( $\beta$ 1–3)GalNAc-epitopes are  $\beta$ -linked in KLH (8), thus ruling out a conventional core 1, *i.e.* Gal( $\beta$ 1–3)GalNAc( $\alpha$ 1-O)Ser/Thr, type of O-glycosylation. To address this question, we have subjected KLH glycopeptides to mild hydrazinolysis conditions, allowing the simultaneous release of both N-linked and O-linked sugar chains (27). Subsequent analysis of the resulting PA-glycans by immunoaffinity chromatography and MALDI-MS disclosed neither further carbohydrate chains nor additional cross-reactive oligosaccharide species (data not shown). Therefore, it may be concluded that the cross-reacting carbohydrate epitope is expressed exclusively by the type of N-glycans described in this study.

Cross-reactive KLH glycans represent, in terms of quantity, minor constituents of this glycoprotein. Nevertheless, KLH acts as an efficient inhibitor of *S. mansoni* infection serum-mediated recognition of schistosomal glycoconjugates and may be also used for serodiagnosis of schistosomiasis. One explanation for this phenomenon might reside in the giant size and heterogeneity of this molecule. KLH consists of two isoforms, KLH1 and KLH2, each of which is composed of several subunits of ~400 kDa. Whereas KLH1 occurs as a cylindrical didecamer, KLH2 forms a mixture of didecamers and tubular multidecamers (2, 3, 48). Each didecamer has a molecular mass of roughly 8,000,000 Da. Because each KLH1 and KLH2 subunit comprises eight and four potential N-glycosylation sites, respectively (EMBL data base: AJ698339 and AJ 698340), sufficient copies of cross-reactive oligosaccharides may exist within each KLH molecule, while representing only minor carbohydrate constituents.

In addition to the Fuc( $\alpha$ 1–3)GalNAc( $\beta$ 1–4)[Fuc( $\alpha$ 1–3)]GlcNAc( $\beta$ 1- epitope, analyzed glycans contained, in part, a xylose residue. This monosaccharide constituent has already been detected in our previous study (21). N-Glycans comprising ( $\beta$ 1–2)-linked xylose are also present in hemocyanins of *Helix pomatia* (49, 50) and *Lymnea stagnalis* (51). In contrast to KLH, however, xylosylated glycans have been reported to represent major carbohydrate constituents of these molecules. Intriguingly, N-glycans with a xylosylated trimannosyl core are also constituents of glycoproteins from *S. mansoni* eggs and cercariae (44, 52). Hence, xylose (1–2)-linked to the central  $\beta$ -mannose represents a second carbohydrate epitope shared by KLH and schistosomal glycoproteins. Insofar, this is remarkable because plant glycoprotein-glycans carrying such ( $\beta$ 1–2)-linked xylose residues have been shown to be immunogenic in animals, in particular in conjunction with ( $\alpha$ 1–3)-linked fucosyl substituents at the innermost GlcNAc of the chitobiose unit (53–55). The question remains open, however, as to whether xylosylated glycan species of KLH may also raise antibodies directed against this sugar moiety. Nevertheless, the detection of xylosylated glycans in KLH highlights again the multifarious glycosylation capacities of *Megathura crenulata* and demonstrates that this organism can be considered a rich reservoir for many, in part, novel glycosyltransferases.

As stated in the introduction, KLH is frequently used as an immunogenic protein carrier for the generation of glycoconjugate vaccines (see, for example Refs. 56 and 57). Because KLH itself carries a number of potentially immunogenic carbohydrate epitopes, resulting carbohy-

drate-specific antibody responses have to be carefully analyzed. In this context, it has been demonstrated, for example, that sera from mice immunized with native KLH or KLH treated with glutaraldehyde cross-reacted with several other carbohydrate antigens like lipoarabinomannan from *Mycobacterium tuberculosis*, glucuronoxylomannan from *Cryptococcus neoformans*, Lewis Y tetrasaccharide, or lipopolysaccharide from *Escherichia coli* serotype O55:B5 (58). Likewise, a strong reaction of sera from *Trichinella* patients with KLH has been described (59), which allows the use of KLH for the diagnosis of both trichinellosis and schistosomiasis and leads to the need of differential diagnosis in areas where both diseases occur (60). The structural basis for this pronounced cross-reactivity of *Trichinella spiralis* infection sera with KLH is not known. The Fuc( $\alpha$ 1–3)GalNAc( $\beta$ 1–4)[Fuc( $\alpha$ 1–3)]GlcNAc( $\beta$ 1- epitope described in this study, however, may provide the basis for the development of neoglycoproteins, which might be useful as highly specific reagents for serodiagnostic purposes.

**Acknowledgments**—We gratefully acknowledge the expert technical assistance of Carolien Koeleman, Peter Kaese, and Werner Mink. We thank Dr. Q. Bickle and Dr. M. J. Doenhoff for supply of antibodies and Dr. J. Markl for providing KLH.

## REFERENCES

- van Holde, K. E., and Miller, K. I. (1995) *Adv. Protein Chem.* **47**, 1–81
- Harris, J. R., and Markl, J. (1999) *Micron* **30**, 597–623
- Harris, J. R., and Markl, J. (2000) *Eur. Urol.* **37**, 24–33
- Jurincic-Winkler, C. D., Metz, K. A., Beuth, J., and Klippel, K. F. (2000) *Eur. Urol.* **37**, 45–49
- Lamm, D. L., Dehaven, J. I., and Riggs, D. R. (2000) *Eur. Urol.* **37**, 41–44
- Mansour, M. A., Ali, P. O., Farid, Z., Simpson, A. J. G., and Woody, J. W. (1989) *Am. J. Trop. Med. Hyg.* **41**, 338–344
- Alves-Brito, C. F., Simpson, A. J. G., Bahia-Oliveira, L. M. G., Rabello, A. L. T., Rocha, R. S., Lambertucci, J. R., Gazzinelli, G., Katz, N., and Correa-Oliveira, R. (1992) *Trans. R. Soc. Trop. Med. Hyg.* **86**, 53–56
- Wirguin, I., Suturkova-Milosevic, L., Briani, C., and Latov, N. (1995) *Cancer Immunol. Immunother.* **40**, 307–310
- Danishesky, S. J., and Allen, J. R. (2000) *Angew. Chem. Int. Ed. Engl.* **39**, 836–863
- Wang, Z. G., Williams, L. J., Zhang, X. F., Zatorski, A., Kudryashov, V., Ragupathi, G., Spassova, M., Bornmann, W., Slovin, S. F., Scher, H. I., Livingston, P. O., Lloyd, K. O., and Danishesky, S. J. (2000) *Proc. Natl. Acad. Sci. U. S. A.* **97**, 2719–2724
- Chapman, P. B., Morrissey, D., Panageas, K. S., Williams, L., Lewis, J. J., Israel, R. J., Hamilton, W. B., and Livingston, P. O. (2000) *Clin. Cancer Res.* **6**, 4658–4662
- Gilewski, T., Adluri, S., Ragupathi, G., Zhang, S., Yao, T. J., Panageas, K., Moynahan, M., Houghton, A., Norton, L., and Livingston, P. O. (2000) *Clin. Cancer Res.* **6**, 1693–1701
- Krug, L. M., Ragupathi, G., Ng, K. K., Hood, C., Jennings, H. J., Guo, Z., Kris, M. G., Miller, V., Pizzo, B., Tyson, L., Baez, V., and Livingston, P. O. (2004) *Clin. Cancer Res.* **10**, 916–923
- Krug, L. M., Ragupathi, G., Hood, C., Kris, M. G., Miller, V. A., Allen, J. R., Keding, S. J., Danishesky, S. J., Gomez, J., Tyson, L., Pizzo, B., Baez, V., and Livingston, P. O. (2004) *Clin. Cancer Res.* **10**, 6094–6100
- Dissous, C., Grzych, J. M., and Capron, A. (1986) *Nature* **323**, 443–445
- Markl, J., Nour el Din, M., Winter-Simanowski, S., and Simanowski, U. A. (1991) *Naturwissenschaften* **78**, 30–31
- Xue, C. G., Taylor, M. G., Bickle, Q. D., Sacoli, and Renaganthan, E. A. (1993) *Trans. R. Soc. Trop. Med. Hyg.* **87**, 654–658
- Taylor, M. G., Huggins, M. C., Shi, F., Lin, J., Tian, E., Ye, P., Shen, W., Qian, C. G., Lin, B. F., and Bickle, Q. D. (1998) *Vaccine* **16**, 1290–1298
- van de Vijver, K. K., Hokke, C. H., van Remoortere, A., Jacobs, W., Deelder, A. M., and Van Marck, E. A. (2004) *Int. J. Parasitol.* **34**, 951–961
- Kurokawa, T., Wuhler, M., Lochnit, G., Geyer, H., Markl, J., and Geyer, R. (2002) *Eur. J. Biochem.* **269**, 5459–5473
- Wuhler, M., Robijn, M. L., Koeleman, C. A., Balog, C. I., Geyer, R., Deelder, A. M., and Hokke, C. H. (2004) *Biochem. J.* **378**, 625–632
- Wuhler, M., Dennis, R. D., Doenhoff, M. J., and Geyer, R. (2000) *Mol. Biochem. Parasitol.* **110**, 237–246
- Kantelhardt, S. R., Wuhler, M., Dennis, R. D., Doenhoff, M. J., Bickle, Q., and Geyer, R. (2002) *Biochem. J.* **366**, 217–223
- Hamilton, J. V., Chiodini, P. L., Fallon, P. G., and Doenhoff, M. J. (1999) *Parasitology*

- 118, 83–89
25. Bickle, Q. D., and Andrews, B. J. (1988) *Parasite Immunol.* **10**, 151–168
26. Hase, S., Ibuki, T., and Ikenaka, T. (1984) *J. Biochem. (Tokyo)* **95**, 197–203
27. Kuraya, N., and Hase, S. (1992) *J. Biochem. (Tokyo)* **112**, 122–126
28. Hase, S. (1994) *Methods Enzymol.* **230**, 225–236
29. Suckau, D., Resemann, A., Schuierenberg, M., Hufnagel, P., Franzen, J., and Holle, A. (2003) *Anal. Bioanal. Chem.* **376**, 952–965
30. Lewandrowski, U., Resemann, A., and Sickmann, A. (2005) *Anal. Chem.* **77**, 3274–3283
31. Wuhrer, M., Koeleman, C. A., Deelder, A. M., and Hokke, C. H. (2004) *Anal. Chem.* **76**, 833–838
32. Geyer, H., Schmitt, S., Wuhrer, M., and Geyer, R. (1999) *Anal. Chem.* **71**, 476–482
33. Haslam, S. M., Coles, G. C., Morris, H. R., and Dell, A. (2000) *Glycobiology* **10**, 223–229
34. Wuhrer, M., Dennis, R. D., Doenhoff, M. J., Bickle, Q., Lochnit, G., and Geyer, R. (1999) *Mol. Biochem. Parasitol.* **103**, 155–169
35. Anumula, K. R. (1994) *Anal. Biochem.* **220**, 275–283
36. Geyer, R., Geyer, H., Kühnhardt, S., Mink, W., and Stirm, S. (1983) *Anal. Biochem.* **133**, 197–207
37. Geyer, R., and Geyer, H. (1994) *Methods Enzymol.* **230**, 86–108
38. Wuhrer, M., Kantelhardt, S. R., Dennis, R. D., Doenhoff, M. J., Lochnit, G., and Geyer, R. (2002) *Eur. J. Biochem.* **269**, 481–493
39. Friedl, C. H., Lochnit, G., Zähringer, U., Bahr, U., and Geyer, R. (2003) *Biochem. J.* **369**, 89–102
40. Harvey, D. J. (1999) *Mass Spectrom. Rev.* **18**, 349–450
41. Mechref, Y., Novotny, M. V., and Krishnan, C. (2003) *Anal. Chem.* **75**, 4895–4903
42. Tretter, V., Altmann, F., and März, L. (1991) *Eur. J. Biochem.* **199**, 647–652
43. Khoo, K. H., Sarda, S., Xu, X., Caulfield, J. P., McNeil, M. R., Homans, S. W., Morris, H. R., and Dell, A. (1995) *J. Biol. Chem.* **270**, 17114–17123
44. Khoo, K. H., Chatterjee, D., Caulfield, J. P., Morris, H. R., and Dell, A. (1997) *Glycobiology* **7**, 663–677
45. Huang, H. H., Tsai, P. L., and Khoo, K. H. (2001) *Glycobiology* **11**, 395–406
46. Robijn, M. L., Wuhrer, M., Kornelis, D., Deelder, A. M., Geyer, R., and Hokke, C. H. (2005) *Parasitology* **130**, 67–77
47. Stoeva, S., Schutz, J., Gebauer, W., Hundsdoerfer, T., Manz, C., Markl, J., and Voelter, W. (1999) *Biochim. Biophys. Acta* **1435**, 94–109
48. Markl, J., Lieb, B., Gebauer, W., Altenhein, B., Meissner, U., and Harris, J. R. (2001) *J. Cancer Res. Clin. Oncol.* **127**, R3–R9
49. van Kuik, J. A., van Halbeek, H., Kamerling, J. P., and Vliegthart, J. F. G. (1985) *J. Biol. Chem.* **260**, 13984–13988
50. Lommerse, J. P., Thomas-Oates, J. E., Gielens, C., Preaux, G., Kamerling, J. P., and Vliegthart, J. F. G. (1997) *Eur. J. Biochem.* **249**, 195–222
51. Van Kuik, J. A., Sijbesma, R. P., Kamerling, J. P., Vliegthart, J. F., and Wood, E. J. (1987) *Eur. J. Biochem.* **169**, 399–411
52. Khoo, K. H., Huang, H. H., and Lee, K. M. (2001) *Glycobiology* **11**, 149–163
53. Lauriere, M., Lauriere, C., Chrispeels, M. J., Johnson, K. D., and Sturm, A. (1989) *Plant Physiol.* **90**, 1182–1188
54. Ueda, H., and Ogawa, H. (1999) *Trends Glycosci. Glycotechnol.* **11**, 413–428
55. Fotisch, K., and Vieths, S. (2001) *Glycoconj. J.* **18**, 373–390
56. Ragupathi, G., Deshpande, P. P., Coltart, D. M., Kim, H. M., Williams, L. J., Danishefsky, S. J., and Livingston, P. O. (2002) *Int. J. Cancer* **99**, 207–212
57. Jansen, W. T., Hogenboom, S., Thijssen, M. J., Kamerling, J. P., Vliegthart, J. F. G., Verhoef, J., Snippe, H., and Verheul, A. F. (2001) *Infect. Immun.* **69**, 787–793
58. May, R. J., Beenhouwer, D. O., and Scharff, M. D. (2003) *J. Immunol.* **171**, 4905–4912
59. Thors, C., and Linder, E. (1998) *Parasite Immunol.* **20**, 489–496
60. Ittiprasert, W., Butraporn, P., Kitikoon, V., Klongkamnuankarn, K., Pholsena, K., Vanisaveth, V., Sakolvaree, Y., Chongsanguan, M., Tapchaisri, P., Mahakunkijchareon, Y., Kurazono, H., Hayashi, H., and Chaicumpa, W. (2000) *Parasitol. Int.* **49**, 209–218
61. Domon, B., and Costello, C. (1988) *Glycoconj. J.* **5**, 397–409
62. Kamerling, J. P., and Vliegthart, J. F. G. (1992) in *Biological Magnetic Resonance: Carbohydrates and Nucleic Acids* (Berliner, L. J., and Reuben, J., eds) pp. 1–194, Plenum Press, New York